ucific Marine Environmental Laboratory

Annual Report for FY 90

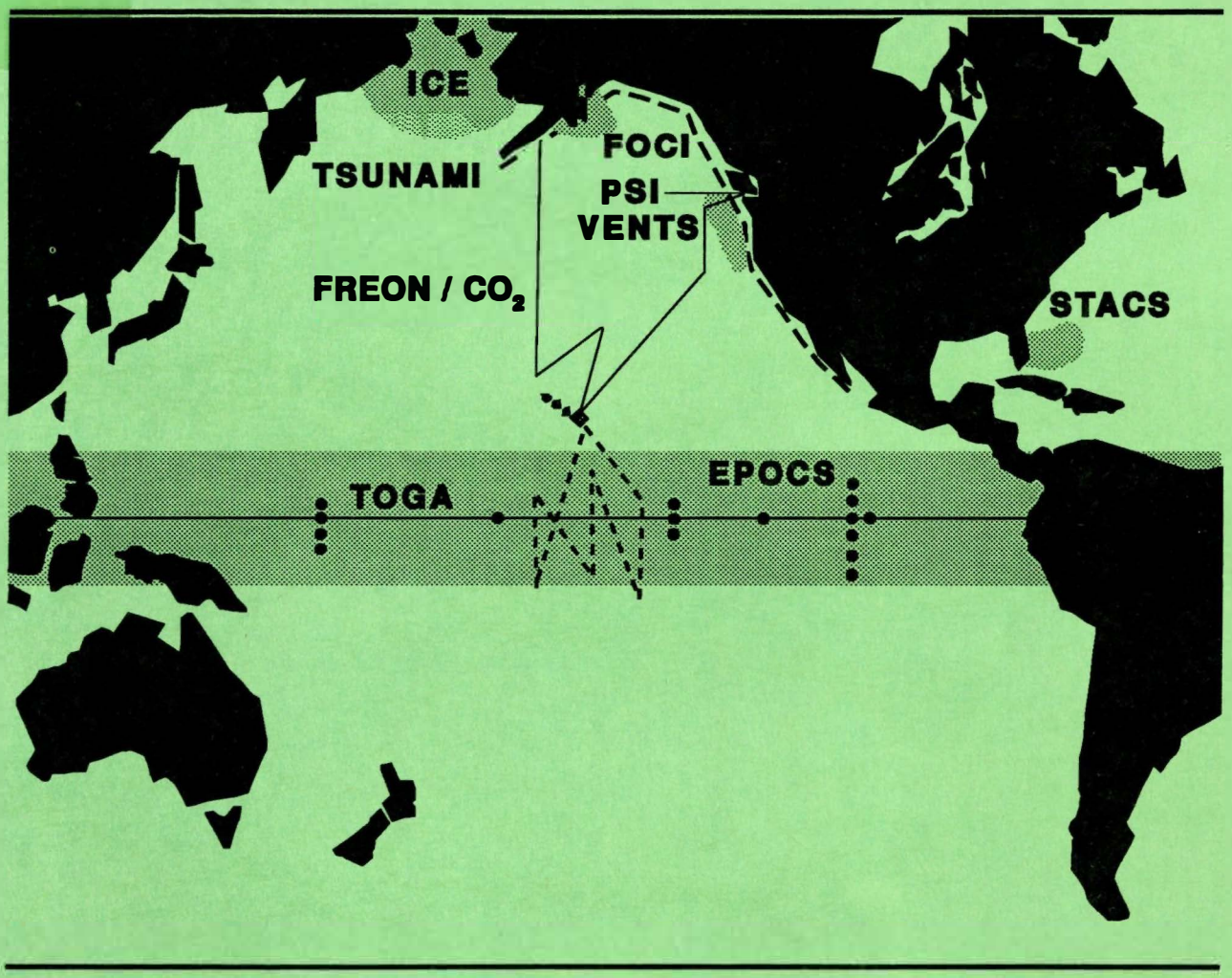

UNITED STATES DEPARTMENT OF COMMERCE

National Oceanic and Atmospheric Administration
Environmental Research Laboratories

PACIFIC MARINE ENVIRONMENTAL LABORATORY ANNUAL REPORT FISCAL YEAR 1990

March 1991

Pacific Marine Environmental Laboratory
7600 Sand Point Way NE
Seattle, WA 98115

UNITED STATES DEPARTMENT OF COMMERCE

Robert A. Mosbacher
Secretary

NATIONAL OCEANIC AND ATMOSPHERIC ADMINISTRATION

John A. Knauss
Under Secretary for Oceans and Atmosphere/Administrator

Environmental Research Laboratories

Joseph O. Fletcher
Director

NOTICE

Mention of a commercial company or product does not constitute an endorsement by NOAA/ERL. Use of information from this publication concerning proprietary products or the tests of such products for publicity or advertising purposes is not authorized.

CONTENTS

INTRODUCTION

E.N. Bernard, Director

The Pacific Marine Environmental Laboratory (PMEL) carries out interdisciplinary scientific investigations in oceanography, marine meteorology, and related subjects. Current PMEL programs focus on climate, marine observation and prediction, marine resources, and marine environmental assessment. Studies are conducted to improve our understanding of the complex physical and geochemical processes that determine the extent of human effect on the marine environment; to define the forcing functions and the processes driving ocean circulation and the global climate system; and to improve environmental forecasting capabilities and other supporting services for marine commerce and fisheries.

PMEL complements its research efforts through two ERL cooperative institutes: the Joint Institute for Study of the Atmosphere and Ocean (JISAO), with the University of Washington; and the Joint Institute for Marine and Atmospheric Research (JIMAR), with the University of Hawaii. PMEL also complements its research through NOAA's National Marine Fisheries Service (NMFS) and the Cooperative Institute for Marine Resources Studies (CIMRS), a joint organization with Oregon State University.

CLIMATE RESEARCH

The National Oceanic and Atmospheric Administration (NOAA) Ocean Climate Program was developed following the passage of the National Climate Program Act in 1978 in response to increased public awareness of the effects of short- and long-term climatic changes and a concern about the potential impact of technology and population growth on world climate. More recently, NOAA has initiated the Climate and Global Change (CGC) Program to study oceanic thermohaline circulation and its climatic impact in coordination with other Federal agencies. These two major NOAA programs form the backbone of much of the research conducted at PMEL.

Understanding and forecasting climatic change requires an understanding of the processes of heat, moisture, and momentum exchange between the ocean and atmosphere as well as the large-scale transports of heat within the atmosphere and ocean. PMEL's climate and global change research program conducts studies of both local and basin-wide ocean dynamics and the coupled ocean-atmosphere circulation, with the goal of determining the physical mechanisms that generate anomalies in sea-surface temperature (SST) distributions in the tropical ocean. A crucial step is to develop and validate ocean circulation models that are capable of simulating the evolution of globally important events such as El Niño.

Man's addition of chemical constituents to the atmosphere and the potential consequences of these changes create a need for improved understanding of the ocean's absorption, transport, and emission of the important trace gases. PMEL research in these areas focuses on the carbon cycle in the ocean-atmosphere system and the air-sea exchange of other radiatively important trace species. These studies involve integrated chemical and physical measurements of the oceanic and atmospheric boundary layer.

Heat transport by major western boundary currents (the Gulf Stream and the Kuroshio in the Northern Hemisphere) is also postulated to have an important effect on world climate. Western boundary current studies at PMEL continue to focus on the Florida Current as part of the Subtropical Atlantic Climate Studies (STACS).

Accomplishments FY 90

EQUATORIAL DYNAMICS

In support of the Equatorial Pacific Ocean Climate Studies (EPOCS) and Tropical Ocean and Global Atmosphere (TOGA) programs, PMEL maintains an array of moored and island stations in the tropical Pacific. Twenty-four moored stations measure the vertical distribution of current velocity, temperature, and salinity between the surface and 500 m on the Equator and the temperature profile down to 500 m off the Equator. The moorings transmit wind velocity, air temperature, SST, currents at 10 m, and the off-equatorial temperature profiles in real time.

Automated wind stations are also maintained on islands in the western and central Pacific (Kapingamarangi, Nauru, Baker, and Christmas Islands). Data from these stations are used to diagnose oceanic and atmospheric processes in the tropical Pacific, to validate the operational general ocean circulation model at the National Meteorological Center (NMC), and to study air-sea interaction processes responsible for annual and interannual variability of the tropical Pacific.

Equatorial SST Variations

A central focus of the TOGA and EPOCS programs is to understand the mechanisms responsible for variations in the equatorial Pacific Ocean on El Niño-Southern Oscillation (ENSO) time and space scales. During 1986–1988, EPOCS, TOGA, and the U.S./People's Republic of China bilateral undertook 12 research cruises and maintained the array of current meter moorings, Automated Temperature Line Acquisition System (ATLAS) wind and thermistor chain moorings, and island wind stations. Data from these and other sources were merged into a comprehensive description of variability on daily to interannual time scales over approximately 100° of longitude (110°W to 155°E) in the equatorial Pacific. As a result of these efforts, the 1986–1988 ENSO event is the best documented ever, based on in-situ wind, ocean current, and temperature data. The descriptive analyses of these data provided the necessary background for more detailed studies now under way in which specific dynamic and thermodynamic hypotheses are being tested. In addition, these analyses have provided the observational framework needed for the design and implementation of a basin-wide, tropical Pacific observing system, the TOGA Tropical Atmosphere-Ocean (TOGA-TAO) array, required for the second half of the TOGA decade. Within this array, detailed process studies will examine dynamic air-sea interactions critical for modeling ENSO.

TOGA-TAO Project Office

In support of the Climate and Global Change Program, the TOGA-TAO Project Office was established jointly by the Oceanic and Atmospheric Research (OAR) and the National Ocean Service (NOS) arms of NOAA. The project office will be responsible for maintaining the TOGA-TAO array, which is planned to include 65 ATLAS moorings spanning the equatorial Pacific from 110°W to 145°E. By the end of FY 90, the array was 29% completed with 19 moorings in place. Expansion of TOGA-TAO is the highest priority for the ocean observing system in the second half of the TOGA decade.

PROTEUS Mooring System

A new mooring system, Profile Telemetry of Upper Ocean Currents (PROTEUS), was developed which has the capability of transmitting profiles of ocean currents in real time, using a moored acoustic Doppler current profiler. This system was successfully deployed on the Equator at 140°W in April 1990 and has operated flawlessly since then. Data from this and other moored arrays are used to study low-frequency dynamics and thermodynamics in the upper equatorial Pacific Ocean.

Modeling of the Tropical Pacific

The effect of westerly wind bursts in the western Pacific on SST in the eastern Pacific was evaluated using the Geophysical Fluid Dynamics Laboratory (GFDL) ocean circulation model. Results indicate that these bursts could be important in the onset of ENSO events. This study also led to an empirical study of island wind data to categorize types of westerly wind events. Both these analyses are critical for the planning of the TOGA Coupled Ocean-Atmosphere Response Experiment (COARE).

WESTERN BOUNDARY CURRENTS

Estimates of transport by the Florida Current are derived from observations of the cross-stream cable voltages between Jupiter, FL, and Settlement Point, Grand Bahama Island. Eight years of data have been scrutinized for errors, edited using improved estimates of the geomagnetic and tidal variations, and adjusted for secular change in the Earth's magnetic field. The new magnetic station at Settlement Point now permits measurement of, and compensation for geomagnetic variations on a daily to weekly basis. Use of similar cable for transport measurements is an integral part of the emerging Atlantic Climate Change Program.

MARINE AND ATMOSPHERIC CHEMISTRY FOR CLIMATE CHANGE

PMEL conducts two important marine chemistry programs for NOAA under the National Climate Program. One program studies how the ocean affects the atmospheric concentration of several climatically important trace species. This study focuses on the biogeochemical cycles of carbon, sulfur, nitrogen, and oxygen. The other program measures the changing concentration of anthropogenic fluorocarbons in the ocean to elucidate pathways and rates of thermocline ventilation and circulation.

Biogeochemical Cycles

PMEL participated in three major field programs in 1990 to study trace gases and aerosols that affect climate.

The third Soviet-American Gas and Aerosol experiment (SAGA-3) was conducted on the Soviet R/V *Akademic Korolev* and included five Equator crossings between Hilo, Hawaii, and American Samoa during February and March. The major objectives of the cruise were to study (1) factors controlling the background photochemistry of the remote tropical marine boundary layer, (2) the flux of biogenic trace gases (CO_2, CH_4, CO, and dimethyl sulfide) from the ocean, and (3) the formation of particles in the remote marine atmosphere.

The second expedition was aboard NOAA Ship *Malcolm Baldrige* along 170°W from Western Samoa to 60°S and north to Hawaii. PMEL measured carbon cycle trace gases (CO_2, CO, and CH_4) in the atmosphere and in surface waters by gas chromatography, filling in some of the major data gaps for the South Pacific that hinder accurate assessment of global carbon fluxes.

The third major field project, the Pacific Sulfur/Stratus Investigation (PSI), is a multiagency (NOAA, NASA, DOE, DOD, NSF) program to study the effect of the sulfur cycle on marine stratus clouds and climate. PSI-2, the second in an annual series, was conducted off the Washington coast in April, and included measurements from NOAA Ship *McArthur*, a coastal research station at Cheeka Peak, and a University of Washington research aircraft.

CFC tracer program

Chlorofluorocarbon (CFC), salinity, temperature, dissolved oxygen, nutrients, carbon dioxide, and helium-tritium were measured on a 2-month-long NOAA Climate and Global Change cruise in the southwest Pacific in the spring of 1990. These measurements document the evolution of CFC transients in the thermocline and intermediate waters of the southwest Pacific since the first NOAA CFC tracer cruise in this region in 1984. CFCs were also detected along the Tonga-Kermadec Ridge and east of New Zealand in the deep western boundary current, which is the major source of inflow into the interior of the deep Pacific. The PMEL CFC tracer group also participated in the World Ocean Circulation Experiment (WOCE) CFC Intercalibration Cruise in December 1989. Careful intercomparisons between PMEL, Scripps Institution of Oceanography (SIO), and Woods Hole Oceanographic Institution (WHOI) CFC groups during this cruise will facilitate the exchange of tracer data sets and aid in collaborative efforts.

Plans FY 91

EQUATORIAL DYNAMICS

- Continue implementation of TOGA-TAO array.
- Continue development and deployment of PROTEUS moorings.
- Complete analysis of the dynamics of the North Equatorial Countercurrent.
- Complete analysis of the annual cycle in the eastern, central, and western equatorial Pacific Ocean.
- Complete studies of the mechanisms of seasonal warming and cooling in the equatorial waveguide, using model and observational data.

WESTERN BOUNDARY CURRENTS

- Continue to improve the cross-stream measurements of the Florida Current.
- Develop a strategy for expanding the use of cables for transport measurements in the Atlantic Climate Change Program.

MARINE AND ATMOSPHERIC CHEMISTRY FOR CLIMATE CHANGE

- Conduct a CO_2/RITS/CFC transect in the northern Pacific Ocean along 150°W in coordination with CGC and WOCE programs.

- Participate in the U.S./Australian WOCE cruises in the tropical and circumpolar regions of the southwestern Pacific Ocean.

- Conduct a pilot study of the ventilation of deep waters in the Greenland-Norwegian Seas, using CFCs and other tracers.

- Conduct a third multiagency PSI study off the Washington coast to study the effect of the marine sulfur cycle on stratus clouds and climate.

MARINE RESOURCES

Accomplishments FY 90

VENTS PROGRAM

The VENTS Program was established in 1984 to focus NOAA interdisciplinary research on the oceanic effects of hydrothermal activity along seafloor spreading centers. At that time, hydrothermal venting had been directly observed by means of submersible along the Galapagos Ridge, the East Pacific Rise, and the Juan de Fuca Ridge. The accelerating rate of spreading-center hydrothermal discoveries has resulted in an increasing recognition of seafloor hydrothermal venting's importance as a fundamental process whereby mass and heat are transferred from the Earth's interior to its surface along the entire 60,000-km-long global spreading-center system.

Recent results from both national and international mid-ocean ridge research projects show that hydrothermal activity along seafloor spreading centers significantly affects oceanic chemical and thermal budgets at scales ranging from local to global. VENTS Program research is directed toward determining, and then understanding, hydrothermal processes that may have large-scale ocean environmental effects, in some cases over periods of years to centuries.

In carrying out this research mission, the VENTS Program strategy has been to focus on a limited, but significant, segment of the global spreading-center system and to study impacts of hydrothermal activity within a single oceanic basin. VENTS research has therefore been concentrated on the isolated seafloor spreading centers in the northeastern Pacific. In FY 90, VENTS research focused on two principal tasks:

- Determination of the patterns and pathways of the regional transport of conservative and nonconservative hydrothermal emissions. This research addresses the composition, variability, and fate of specific hydrothermal chemicals, minerals, and gases that are both dissolved and suspended in hydrothermal effluent, as well as the chemical, physical, and biological reactions associated with hydrothermal fluids that result in the removal of certain elements from seawater.

- Determination of the source strengths of hydrothermal emissions and their relationships to volcanological and tectonic factors that influence the location, vigor, and duration of hydrothermal venting.

Transport of Hydrothermal Emissions

An intensive surface ship and submersible program was carried out to map the distributions of hydrothermally derived Si, ^3He, Mn, Fe, CO_2, and heat along the ridge axis of Cleft Segment. Results show that hydrothermal emissions from the southern Juan de Fuca Ridge form an elongated plume, recognizable several tens of kilometers beyond the ridge crest by unique

elemental signatures in suspended particles. Fe- and P-enriched particulate matter were traced more than 50 km to the west along the southern edge of the Vance Seamount chain. A similar hydrothermal plume has been observed southwest of the Endeavour Segment. It is possible that these plumes coalesce west of the Cobb-Eickelberg Seamount to form the hydrothermal "megaplume" that extends west of the ridge axis for at least 1,500 km.

Comprehensive analysis of the hydrothermal particulates indicates that phosphorus is being scavenged from solution by the newly formed iron oxyhydroxides, which settle to the seafloor. Similarly, geochemical evidence for scavenging of vanadium, chromium, and arsenic by hydrothermal iron oxides was also observed in the water column and underlying sediments. These findings demonstrate the important role of hydrothermal emissions as scavengers of chemicals from seawater. Mass balance calculations suggest that hydrothermal emissions account for approximately 10–30% of the phosphorus sinks in the oceans.

During FY 90, work began on the development of an in-situ chemical analysis system designed to operate in a real-time scanning mode in order to map the distribution of iron and manganese in seawater/vent fluid mixtures as a function of vent temperature. Vent water composition and temperature are key parameters that affect chemical reactions in the hydrothermal plumes.

The first systematic investigation of zooplankton biology in a neutrally buoyant hydrothermal plume was completed. In collaboration with VENTS scientists, researchers from Woods Hole Oceanographic Institution made six near-bottom tows through the megaplume vent field. The primary goal of this research was to test the hypothesis that hydrothermal plumes are effective dispersal agents for the larvae of benthic vent animals.

Eleven moorings were deployed around the megaplume vent field to study temporal variability of venting, integrated heat flux from the field, and the near-field deposition of hydrothermal particles. The moored instruments included 44 current meters, 20 sediment traps, and 9 transmissometers.

Long-term moored-array current measurements show that plumes may be advected along the Cleft Segment of the southern Juan de Fuca Ridge before being deflected west or east by bathymetric features such as the Cobb-Eickelberg Seamount chain or the Vance Volcanoes Chain. The background flow into which plumes are ejected is more energetic than expected, and variations can reverse flows on several different time scales. Temperature variations with periods of 1–2 months can be as large as plume thermal anomalies.

A three-dimensional map was made of the neutrally buoyant warm plume overlying the megaplume vent field. The plume was mapped around and within the moored array in order to obtain a high-resolution initial description of the plume that will be monitored over year-long intervals by the moored instruments.

Source Strengths of Hydrothermal Emissions

Geological surveys carried out during the VENTS FY 90 *Alvin* dives on the southern Juan de Fuca Ridge resulted in the discovery of an extensive high-temperature hydrothermal vent field

that appears to be the source of the megaplume, a very large, steady-state hydrothermal plume observed in this region for the past several years.

Other dives confirmed the existence of a new volcanic mound on the seafloor in the megaplume region. The mound was first noted as a bathymetric discrepancy in a comparison of VENTS Sea Beam maps compiled in 1981 and newer maps resulting from repeat surveys carried out in 1987. The volcanic activity that created this mound may have been associated with the generation of the 1986 megaplume events.

Results from the second year of the bottom pressure recorder (BPR) experiment at Axial Volcano showed no obvious evidence of volcanic deflation. One observed event, which is too small to be positively identified as deflation, emphasizes the need for enhanced, multi-sensor monitors. Data from a third-year BPR deployment are currently under analysis.

An analysis system for classifying seafloor terrain, based on the spectral content of Sea Beam bathymetry, was developed and is currently being applied to the Juan de Fuca Ridge. In addition, a terrain correction system for sidescan sonar imaging was developed and is being tested. A data base system for all VENTS Sea Beam bathymetry was implemented and allows ready access to all such data for use in contour mapping.

A surface gravity and magnetics survey of the southern Juan de Fuca Ridge was successfully completed from the NOAA Ship *Discoverer*. The area covered included Cleft and Vance Segments and was especially centered on the source region of the megaplume events.

During FY 90, studies were completed on the magnetic properties of rocks and modeling of magnetic lows at the Sea Cliff hydrothermal field on the northern Gorda Ridge. The studies support the original interpretation that the magnetic lows are produced primarily by hydrothermal alteration of the magnetic mineral component of basaltic rocks.

During FY 90, permission was granted by the U.S. Navy for VENTS to access certain SOFAR hydrophone arrays for the purpose of establishing an event detection system capable of determining when and where episodic events such as submarine volcanic eruptions and megaplume bursts occur. Detailed plans for the detection instrumentation have been provided to the Navy, and initial equipment installation is expected to begin as early as January 1991.

FISHERIES OCEANOGRAPHY COORDINATED INVESTIGATIONS (FOCI)

Effective management of the commercially valuable stocks of pollock (*Theragra chalcogramma*) in Alaskan waters could be improved with better knowledge of how coupled physical-biological interactions affect year-to-year changes in recruitment. The goal of FOCI is to understand the processes that lead to variations in fishery recruitment. Research was conducted in support of the paradigm that such variations occur as a result of events during fishes' early life history. Our focus has been to elucidate physical and biological phenomena and to understand how complex interactions between these two phenomena affect rates of mortality.

To date, nearly all research has been conducted in the Shelikof Strait region of the Gulf of Alaska. This stock of pollock was selected because it met the criteria of being commercially important and having a tractable early life history.

During FY 90, seasonal and interseasonal variation of pollock in the western Gulf of Alaska was examined using 5 years of current, water discharge, and climatological data. An important finding was that an index of storm activity in the northeastern Pacific (northeastern Pacific pressure index) has important regional manifestations in both winds and currents. Thus there is a direct link between this climate-scale function and local physics. This helps to establish a cause-and-effect basis for the relationship between the pressure index and the abundance of adult pollock.

A model of time-dependent larval dispersion was used to simulate observations. There were two surveys of larval pollock in spring 1988. The first survey data were used as an initial condition, together with estimates of advection and diffusion, to generate a prediction of the distribution of larvae observed during the second survey. The success of this approach clearly indicates the importance of improving our knowledge of the velocity field input.

The fate of larvae carried into the Gulf of Alaska by the Alaska Coastal Current has been elucidated. Between 1986 and 1987, 26 satellite-tracked buoys were drogued at 40 m in the vicinity of the highest concentration of spawning; 17 buoys remained over the continental shelf and 9 buoys were transported off the shelf and entered the oceanic Alaskan Stream. The off-shelf buoy trajectories showed a well-formed, narrow, high-speed current. All but one of the buoys went aground in the Aleutian Islands or entered the southern Bering Sea. Larvae that follow a similar path would probably be lost to recruitment in the Gulf of Alaska stock. Additional observations in the Alaskan Stream have revealed a narrow, extremely stable flow. This result has helped to verify previous inferences and is in excellent agreement with a recent hydrodynamic model of the northeastern Pacific Ocean.

Most of the pollock larvae remain on the Gulf of Alaska shelf. How they are retained and what factors affect their survival are important PMEL research topics. During spring 1990, three satellite-tracked buoys deployed in a high-density patch of larval pollock were caught in an eddy. This was the first time buoys had clearly described such a marked feature in the circulation of the region. Speeds around the eddy were 20 to 30 cm s^{-1}, and the eddy had an apparent diameter of 25 km. After remaining stationary for many days, the eddy began to move southwestward, lose rotational energy, and apparently dissipate as the waters shoaled. The three buoys passed through the Semidi Islands and continued along the coast. It is in such coastal waters that the highest concentrations of young-of-the-year fish have been observed in the past.

FOCI began to implement a new data management and analysis system, known as Extensive PMEL Information Collection (EPIC). This system allows efficient access to many forms of data, including traditional physical oceanographic observations, and less standard biological observations. EPIC also permits easy implementation and use of modern analysis programs and display routines.

Plans FY 91

VENTS PROGRAM

- Reduce and analyze the current meter, sediment trap, and transmissometer data sets obtained during the FY 90 mooring experiment at the megaplume vent field.

- Continue the decadal-scale monitoring of venting variability on the Cleft Segment of the Juan de Fuca Ridge.

- Conduct reconnaissance surveys of venting activity on the north and south Axial Volcano rift zones.

- Undertake a synthesis of venting distribution and geologic structure along the Juan de Fuca Ridge in order to understand the large-scale control exerted by geology on the occurrence of venting.

- Integrate off-axis CTD observations and current meter measurements collected over the past several years in order to determine a regional circulation pattern and its variability.

- Conduct an *Alvin* dive at Cleft Segment, Juan de Fuca Ridge, with the objectives of describing high-temperature venting chemistry and modeling the mixing behavior of seawater with heat and major elements in hydrothermal fluids within the buoyant plume.

- Continue the development of in-situ, scanner-mode measurements of the concentrations of dissolved Mn, Fe, and Si in vent fluids and hydrothermal plumes.

- Continue analyses of heat-^{3}He-Si relationships in off-axis regions to determine the effects of steady-state and episodic venting on the regional distributions of these constituents in the North Pacific.

- Analyze sediment trap materials for major and trace elements, and determine chemical fluxes to the sediments in on- and off-axis regions west of the Juan de Fuca Ridge.

- Compare bottom roughness statistics derived from Sea Beam backscatter information with those generated by spectral techniques and fractal measures.

- Analyze data from the FY-90 test of the newly-developed enhanced BPR (E-BPR), which incorporates three pressure sensors to account for drift, short baseline tilt sensors, a time-integrating vertical-axis seismometer, and a dynamic pressure gauge to monitor harmonic tremor.

- Deploy the gravimeter-based instrument and four E-BPRs equipped with electromagnetic current meters to monitor a 40-km length of the Cleft Segment.

- Continue development of a semi-quantitative model of the behavior of a phase-separated reservoir at the Axial Seamount Hydrothermal Emissions Study (ASHES) vent field in

collaboration with a postdoctoral student in the Civil Engineering Deptartment at Oregon State University.

- Continue implementation of a T-phase event detection system in collaboration with the U.S. Navy.

- Conduct 20 *Alvin* dives at the megaplume site for the purpose of establishing the relationships between the newly discovered high-temperature venting, a new constructional volcanic mound, and the generation of megaplume events.

FISHERIES OCEANOGRAPHY COORDINATED INVESTIGATIONS (FOCI)

- Adapt a hydrodynamic model to the topological constraints of the Shelikof Strait region and begin initial testing.

- Conduct a field experiment to provide upstream boundary conditions for the hydrodynamic model and observations in interior regions for verification of results from this model.

- Continue long-term observations, including water properties, currents, pollock eggs, larvae; continue acquisition and processing of satellite images.

- Provide measurements of water properties and motion for process-oriented studies of survival and secondary production within a larval patch.

- Begin a Bering Sea FOCI program. Emphasis will be on describing and modeling the general circulation over the basin. A cruise will be conducted jointly with Soviet scientists to provide the first synoptic view of the major transport features and flow through the deep western passes. Detailed data on nutrient distributions will also be obtained.

MARINE OBSERVATION AND PREDICTION

Accomplishments FY 90

ARCTIC RESEARCH

Exchanges through Barrow Canyon

The analysis of recent measurements in Barrow Canyon and supporting oceanographic and meteorological time series was completed. No hypersaline plumes, such as would be expected to result from intensive sea ice formation along the Alaskan coast, were observed to exit through Barrow Canyon during the intensive measurement year 1986–1987. Instead, cold and fresh waters advected down-canyon by the mean flow alternated with up-canyon flow of warm and saline water upwelled onto the shelf. At times the latter resulted in onshore heat and salt fluxes large enough to be of possible local significance, e.g., to the surface heat budget. Contrary to earlier findings, the flow was only weakly correlated with the wind and the atmospheric pressure gradient. Instead, both upwelling and flow reversals were coherent along the shelf at sites 400 km apart, with phase differences corresponding to a speed of 2.3 m s^{-1}. The majority of these events therefore appear to be manifestations of remotely forced shelf waves propagating eastward along the Arctic Ocean margin.

Investigations in the Greenland Sea

The Greenland Sea is one of the few regions in the world capable of ventilating the deep ocean. Of particular interest is the role of the western boundary current in supplying the deep Atlantic's interior region with buoyancy and salt, thereby controlling both the surface-driven convective regime and deep mixing. To assess the supply of buoyancy, two instrumented moorings were recovered and a new one deployed in the recirculation region of the southern Greenland Sea. Meanwhile, analysis of recent data sets concentrated on the contribution of saline sources to the deep mixing regime. Multiple sources of slightly different density, all originating in the Arctic Ocean, can be shown to compete with the cold and fresh deep water produced in the central convective gyre of the Greenland Sea to determine the deep structure of the basins that overflow into the North Atlantic. During most of the 1980s, a failure to drive deep convection in the Greenland Sea has resulted in a significant warming and a slight salinization of the deep water in the formative region.

Joint U.S./U.S.S.R. Chukchi Sea Circulation Study

Plans for a joint U.S./U.S.S.R. field investigation of the shelf circulation from Bering Strait northward are being implemented with two cruises during the latter part of the 1990 field season, one on the *Professor Khromov* and the other on the *Surveyor*. Sixteen instrumented moorings were deployed for a year to provide a detailed time history of currents, sea surface elevation, temperature, and salinity. In addition, each cruise conducted extensive mapping of

water properties, including nutrients and dissolved oxygen and a number of trace substances such as chlorinated organics and stable isotopes. Satellite-tracked surface buoys were used to determine ice drift and meteorological forcing. This joint research program will provide the first comprehensive measurements of a vital arctic shelf area, which has one of the largest biological production rates in the world and which plays a pivotal role in the climatology of the Arctic Ocean.

TSUNAMIS

The primary objective of the PMEL Tsunami Project is an improved understanding of the dynamics of tsunami generation, propagation, and shoreline inundation. To meet this objective, the Pacific Tsunami Observation Program (PacTOP) was established to provide high-quality tsunami measurements in the deep ocean and coastal environment. Three oceanographic cruises were carried out this year to recover and re-deploy bottom pressure recorders (BPRs) as part of the continuous PacTOP network maintenance.

A comparison of PacTOP tsunami measurements with numerical simulations was completed in collaboration with JIMAR scientists. A finite-difference implementation of the nonlinear shallow water equations was used; source terms were based on a rectangular fault plane model of seafloor deformation. This study is the first comparison of a generation/propagation model with truly appropriate field observations, and deals with two small tsunamis generated in the Gulf of Alaska on 30 November 1987 and 6 March 1988; the results illustrate the sensitivity of such tsunami models to errors in source specification.

More recently, another small tsunami was generated on 5 April 1990 by a magnitude 7.6 earthquake in the Marianas Trench. Remarkably, a tsunami wave packet less than 0.5 cm in amplitude was clearly measured by a PacTOP instrument situated more than 800 km distant from the source.

Plans FY 91

ARCTIC RESEARCH

- As part of the Atlantic Climate Change Program, begin monitoring the fresh water flux from the Arctic Ocean through Fram Strait.

- Complete the first set of cruises in the Chukchi Sea in support of the Joint U.S./U.S.S.R. circulation study, and calibrate and process the resulting hydrographic data sets.

TSUNAMIS

- Complete a detailed comparison of existing analytic theories with tsunami waveform measurements.

- Maintain the PacTOP network by the recovery and re-deployment of all deep-ocean BPRs.

MARINE ENVIRONMENTAL ASSESSMENT

Accomplishments FY 90

BIOGEOCHEMISTRY

During 1990, two biogeochemical studies were undertaken on copper (Cu) cycling in marine systems to address problems associated with trace metal pollution including toxic and noxious algal blooms. In the first study, a cathodic stripping voltametry technique (CVS) was improved and tested in Puget Sound. Preliminary results showed three maxima in Cu-complexing ligands in the near surface; at 50 m, the depth of the West Point Sewage Treatment Plant's outfall, which is located just north of the sampling site; and at the bottom. The ligand concentrations and the stability constants were comparable with other coastal water determinations by investigators using cupric ion bioassay and Sep-Pak equilibration. It is apparent that 99% of the dissolved Cu is complexed with organic matter. A model of Cu complexation will contribute to determining whether Cu availability is regulating the severity and frequency of toxic and noxious alga blooms, which have become major problems in many regions of North America.

In the second study, the role that complexation plays in controlling the fate of anthropogenic Cu in estuaries was investigated in a series of radiochemical experiments. The results indicate tha biological processes are controlling the adsorption of Cu, either by active biological uptake o Cu or the excretion of Cu-complexing ligands. Cu adsorption onto particles controls the fate o anthropogenic Cu discharge into marine environments, a subject of considerable interest withi the Toxic Chemical Contaminants component of the Coastal Ocean Program.

Estuarine Circulation Modeling

A principal accomplishment over the past 12 months has been the development and use c models of physical and chemical processes in estuaries, which are central to the goals of th Coastal Ocean Program. Models of time-dependent estuarine circulation and chemica scavenging have been completed. Model distributions have been compared with observation both to evaluate model parameters and to check model completeness and accuracy.

The main focus has been on modeling the fluid circulation of Puget Sound. Intrusions of dens water, important to bottom-water renewal in Puget Sound, were shown to be controlled by fou factors: the horizontal salinity difference across the sill region, the intensity of mixing there, th supply of riverine discharge in the inlet, and the strength and direction of the wind. The mod suggests that a difference in salinity of at least 1.3‰ between the entrance and inner lip of th landward sill is required for the initiation of an intrusion. This difference depends on th entrance salinity, controlled by winds in the Strait of Juan de Fuca and along the coast, and c the salinity in the basin, regulated by run-off and earlier density intrusions. About 20% of th runoff during the winter months is retained in the main basin, freshening it as much as 0.8% As the salinity of the main basin declines in the spring months, the salinity outside the entranc rises toward a summer peak, and the cross-sill salinity gradient reaches a maximum. Th

phenomenon coupled with reduced summertime river runoff, a factor in regulating intrusions, explains why the strongest intrusions occur during the summer.

Surprisingly, vertical mixing at the Admiralty Inlet entrance is advective rather than turbulently diffusive and occurs every tidal cycle, providing a mechanism for surface freshets to dilute bottom water. This weakens the effective cross-sill salinity gradient and dampens the intrusion, an effect not recognized previously in Puget Sound.

Winds affect intrusions in a number of ways besides their effects on the entrance salinity already mentioned. Northward winds transport surface water out of the estuary with a compensating landward bottom flow that hastens the dense-water traverse of the sill region. Southward winds have the opposite effect.

Particulate exchange rates and time scales in Puget Sound were modeled by an analysis of radioisotope data. Particulates were estimated to sediment vertically to a depth of 220 m, in 10–15 days. These are the first such data for an estuary and are an important step toward a complete model of contaminant transport and fate. The values were integrated into a preliminary model of the water column distribution of the "unresolved complex mixture of hydrocarbons" (UCM), a chemical marker of anthropogenic input of material into Puget Sound.

Knowledge of the particulate exchange rates has also allowed the creation of a preliminary model to simulate vertical profiles of small and large particle concentrations as measured optically and fluxes as measured by sediment traps. This will lead to an understanding and quantification of contaminant transport in the coastal ocean, and is one of the Laboratory's contributions to improving the environmental health of the nation.

Chemical Modeling

A model of trace metal behavior in water masses moving along the bottom of deep estuaries has been applied to manganese (Mn) in the main basin of Puget Sound. The model shows that the concentration of dissolved Mn, an important scavenger of toxic metal contaminants in the water column, tends toward a concentration near the bottom that is controlled by the outflux of dissolved Mn from the underlying sediment and the oxidation rate onto particles in the water column. The instantaneous concentration of particulate Mn varies greatly near the bottom as near-bottom currents periodically resuspend metal-bearing bottom sediment. This research contributes to the understanding of the behavior of estuarine contaminants, an element in the NOAA Coastal Ocean Program.

Tidal Currents

Also contributing to the understanding of processes affecting estuarine contaminants, an analysis of tidal currents in the southern reaches of the main basin of Puget Sound shows that the diurnal currents increase in strength toward the bottom. This region includes the southern part of East Passage, heavily contaminated Commencement Bay, and the deeper parts of Dalco Passage. Both the amplitudes and phases of these currents are very sensitive to the density variations in

Puget Sound, causing the tidal currents and their effects on contaminants to vary substantially in time. During rare summer conditions when the water is vertically homogeneous, these currents become uniform with depth.

Sea Level Climatology

In support of both the physical impacts element of the NOAA Coastal Ocean Program and the NOAA and Climate Global Change Program, an ongoing study of sea level variations shows that sea level fluctuations observed in Puget Sound propagate into the Sound from the Pacific Coastal region. For signals with periods greater than those of the tides, the squared coherence is greater than 0.95 between observed sea level at Seattle in Puget Sound and that observed at Neah Bay, near the coast. There is a landward decrease in the amplitudes of these signals (20% decrease at Seattle), due possibly to the spreading of the signals throughout the extensive inland waters of the region. The 90-year time series at Seattle is therefore a useful surrogate for coastal sea level and, indirectly, the historical weather and steric ocean (e.g., El Niño) signals since these are the main causes of sea level variations along the U.S. West Coast.

Plans FY 91

- Complete Mn precipitation studies and apply to dynamical chemical models for estuaries.
- Investigate density intrusions during summer months, using a numerical model.
- Implement a scavenging model of suspended matter that describes profiles, fluxes, and resuspensions of interactive size classes.
- Analyze sea level in Puget Sound for the period 1899–1988 including extreme events, interannual variations, and trends.

JIMAR

The Joint Institute for Marine and Atmospheric Research (JIMAR) was formed in 1977 by a Memorandum of Understanding between NOAA and the University of Hawaii. JIMAR is located at the University of Hawaii at Manoa and is part of the School of Ocean and Earth Sciences and Technology. The principal research interests of JIMAR are equatorial oceanography, climate and global change, tsunamis, and fisheries oceanography.

Accomplishments FY 90

EQUATORIAL OCEANOGRAPHY AND CLIMATE RESEARCH

Western Equatorial Pacific Ocean Circulation Study (WEPOCS)

WEPOCS was a joint U.S.-Australian program to study water mass distributions and circulation in the near-equatorial region north of New Guinea. All WEPOCS III data have been finalized, and an overview paper has been completed on these observations. Analyses of WEPOCS I and II observations of water masses, currents in the Vitiaz Strait, and structure of the "warm pool" mixed layer were completed and documented.

Coupled Ocean-Atmosphere Response Experiment (COARE)

COARE is a program to understand the physical processes that maintain and perturb the warm pool in the western Pacific Ocean. Understanding the coupling between the ocean and atmosphere in this region is the major goal for the second half of the Tropical Ocean and Global Atmosphere (TOGA) program.

COARE planning continued and the COARE Science Plan was completed. A proposal for monitoring the thermohaline structure of the warm pool was submitted.

Hawaiian Ocean Time Series (HOT)

A deep-water station 100 km north of Oahu is occupied monthly to collect physical and biological data for World Ocean Circulation Experiments (WOCE) and the Global Ocean Flux Study. JIMAR has been responsible for both hydrographic measurements and acoustic Doppler current profiling (ADCP) for this program. Data collection continued throughout the year.

Indo-Pacific Sea Level Network and TOGA Sea Level Center

Eighty-one Pacific stations (of 90 proposed for TOGA) and 18 (of 24) Indian Ocean stations are now operating. Hourly, daily, and monthly data are archived at the TOGA Sea Level Center.

Data return from the Pacific is very good, much of it coming in near-real time via satellite. Data return from the newer Indian Ocean network is slow. Monthly maps of Pacific sea level are produced and distributed with about a 1-month lag. Sea level data are being compared with satellite altimeter data from GEOSAT, in anticipation of the TOPEX/POSEIDON altimeter data.

Sea level data are being used in conjunction with other oceanic and atmospheric data sets to study both intraseasonal and interannual variability.

Modeling and Analysis

The effect of nonlinear heating on moist atmospheric Kelvin waves was modeled. Empirical studies of the evolution and vertical structure of the El Niño-Southern Oscillation (ENSO) anomaly mode in the tropical atmosphere were done. Model studies in the β-drift baroclinic vortices were made. Analysis of deep equatorial currents is continuing. The 16-month Pacific Equatorial Ocean Dynamics (PEQUOD) data show vertical mean (barotropic) flows of about 2 cm^{-1}, on meridional scales characteristic of baroclinic disturbances.

FISHERIES OCEANOGRAPHY

Seamount Oceanography

Fieldwork involving Doppler Current Profiling and hydroacoustic scattering around Hancock Seamount has been completed. Analysis of the data is under way to relate circulation over seamounts to fisheries productivity.

Island-Flow Interactions and Recruitment

Lobster larvae sampling has been conducted in the Hawaiian archipelago, along with ADCP and other oceanographic data collection. Analysis continued, to investigate the relationship between larval distributions, adult abundances, topography, and currents.

North Pacific Transition Zone

Both physical and biological measurements were obtained on transects in the North Pacific Transition Zone to help assess the effect of large-mesh fishing on pelagic fishes and marine turtles.

TSUNAMI RESEARCH

Inundation Maps

The project to update tsunami inundation and evacuation maps for the State of Hawaii continued. Most of the work on the inundation maps is complete. Work continued on methods for run-up prediction and validation.

Tsunami Modeling

Numerical simulations of tsunamis using a variety of source configurations were computed, and the results were compared with the open-ocean deep pressure observations from the Pacific Tsunami Observation Program (PacTOP). Shallow water equation codes have been used for this purpose. Calculation of inundation began, using both shallow water and fully three-dimensional Navier-Stokes codes.

Plans FY 91

EQUATORIAL OCEANOGRAPHY AND CLIMATE RESEARCH

- Analysis of WEPOCS data will continue. A WEPOCS workshop is planned for spring 1991, to begin model-data intercomparison.

- COARE planning will emphasize final development of an experimental design for the field work.

- In collaboration with PMEL, conductivity sensors will be added to selected TOGA moorings so that space and time scales of the wind, temperature, and salinity of the western Pacific warm pool can be studied.

- Carbon dioxide measurements will be added to the ongoing HOT cruise program, as part of the Climate and Global Change Program.

- The Sea Level Network and TOGA Sea Level Center will continue to archive data, handle data requests, and use the data for research. The emphasis in FY 91 will be on refining altimeter corrections for water vapor and intense rainfall.

- Empirical studies of ENSO variability will be expanded from the equatorial wave guide to the global tropics and extended back to cover a 40-year period.

- A study to compare satellite-based rainfall estimates with ground-truth measurements from rain gauges and radar will be carried out for the Climate and Global Change Program, in preparation for analysis of the upcoming Tropical Rainfall Measuring Mission (TRMM) data.

FISHERIES OCEANOGRAPHY

- Analysis of the Hancock Seamount data will be completed and written up for publication.

- A cruise will go to Palmyra Atoll to deploy drifting buoys, conduct Doppler profiling, and take biological samples.

- An oceanographic data base for the North Pacific Transition Zone data will be set up as a first step in establishing an oceanographic data "library" at the University of Hawaii. This JIMAR facility will be part of a NOAA-National Ocean Survey (NOS) network operating from the Center for Ocean Analysis and Prediction (COAP) in Monterey.

TSUNAMI RESEARCH

- The State of Hawaii inundation maps will be completed. The corresponding evacuation zones will be determined in cooperation with civil defense officials on each island. New techniques for detecting tsunamigenic earthquakes by ionospheric and infrasonic techniques will be explored.

- Numerical modeling of the tsunami run-up using shallow water and Navier-Stokes codes will continue. The aim is to develop the capability for accurate inundation predictions. This is the beginning of JIMAR's effort in the Tsunami Inundation Program (TIP), designed to bring the tsunami warning process to the same state of sophistication as NOAA's storm surge program.

JISAO

The Joint Institute for Study of the Atmosphere and Ocean (JISAO) was established to foster collaboration between NOAA and the University of Washington (UW). JISAO serves as a vehicle for funding grants and postdoctoral Fellows, and supporting collaborative research between NOAA and university scientists. During the past few years, JISAO has emphasized three core research areas: climate, environmental chemistry, and estuaries. Only the climate program has been block funded, and includes more than two-thirds of JISAO's work.

JISAO's climate research has tended to focus on two main themes: large-scale atmosphere-ocean interaction in the tropics, and planetary-scale wave and mean flow interaction. These emphases have served to promote collaboration between the Pacific Marine Environmental Laboratory and university scientists involved in the Equatorial Pacific Ocean Climate Studies (EPOCS) program. JISAO has also been active in directing interdisciplinary research toward an understanding of the global climate system and its sensitivity to human activities. The new Environmental Climate Forecast Center within JISAO was established for this purpose.

The main research themes in environmental chemistry include marine aspects of the carbon dioxide budget, organic carbon dynamics, and chemical processes involving the deposition of heavy metals. This work, particularly the studies of heavy metals, are closely related to ongoing estuarine research efforts. Recently, JISAO's chemistry research has broadened in scope to include other biogeochemical cycles of interest for global climate studies. Of particular interest is the chemistry of sulfur and its influence on cloud condensation nuclei and the cycles that involve long-lived radiatively interactive trace species such as nitrous oxide and methane.

Accomplishments FY 90

JISAO scientists, in collaboration with NOAA scientists, were involved in a variety of climate research activities. They explored the sensitivity of interannual variability in a coupled ocean-atmosphere model to physics parameterizations and climatological mean conditions, giving particular attention to identifying the stability of the coupled tropical ocean-atmosphere system. They also worked on the potential effect of cloud radiation feedback on the El Niño-Southern Oscillation (ENSO) phenomenon and formulated a consistent yet simple model for tropical surface winds. Members of the Environmental Climate Forecast Center contributed to the definition of a TOGA program on seasonal to interannual predictions and to a document summarizing TOGA at its midlife.

Research concerning the propagation of equatorial waves also continued. In particular, researchers investigated the propagation of these waves in the presence of mean currents, studied the propagation of equatorial Kelvin waves on a sloping thermocline, investigated how a coastal Kelvin wave can propagate on a sphere, and completed a study on aspects of Kelvin wave response to episodic wind forcing. Analyses aimed at clarifying the various mechanisms of oscillation in coupled ocean-atmosphere models also continued, along with experiments using

simple delayed-oscillator models, to clear up points relating to the effect of stochastic forcing on the periodicity of such systems.

JISAO's Experimental Climate Forecast Center began operation in January 1989. A computer system was acquired and work began on two problems: (1) exploring the predictability of the ENSO phenomenon, and (2) examining factors that influence climate change on time scales of 100 years.

Research in environmental chemistry included participation in NOAA's Pacific Stratus/Sulfur Investigations (PSI) cruise off the Washington coast, measuring particle size distributions and cloud condensation nucleus spectra. This work has the long-term goal of relating gaseous sulfur emissions by the ocean to particle number or mass concentration of condensation nuclei.

Investigation into the chemistry of vent fluids and their entrainment into hydrothermal plumes continued at Axial Seamount and Juan de Fuca Ridge.

JISAO Supported Workshop

JISAO will provide partial funding for a joint University of Washington-Princeton University course entitled Ocean Circulation: Dynamics and Geochemical Cycling. The seminar will be offered during summer 1991 at the University of Washington Laboratory Facilities at Friday Harbor, Washington. Graduate students from the United States, Japan, France, England, Switzerland, and Germany will participate. A number of scientists from the University of Washington and other institutions will visit and make informal contributions.

Interdisciplinary Initiative

JISAO coordinated and provided administrative support for submission of an interdisciplinary-initiative proposal to the Office of the UW Provost, "Program for UW Research on the Carbon Cycles and Climate Change," for which funding was granted. These funds are providing summer fellowships to seven competetively selected graduate research assistants, as well as equipment and supplies for related projects.

Plans FY 91

- Continue vigorous postdoctoral, visitor, and seminar programs.
- Continue to work with NOAA to expand programs dealing with scientific issues relating to global climate change.
- Continue research on the predictability of El Niño-Southern Oscillation (ENSO) events.
- Continue research on climate, focusing on coupled atmosphere-ocean interaction and biogeochemical cycles.

- Continue participation in research efforts involving EPOCS, Climate and Global Change, and Pacific Sulfur/Stratus Investigations (PSI).

- Host the U.S.-Japan Bilateral Meeting at UW in September 1990.

CIMRS

The Cooperative Institute for Marine Resources Studies (CIMRS) was established in 1982 to foster collaborative research between NOAA and Oregon State University in the areas of oceanography, fisheries, aquaculture and other marine-related fields and to serve as a center at which researchers may address problems of mutual interest relating to the living and non-living components of the marine and estuarine environment and their interrelationships. Oregon State University is currently involved in research efforts that parallel NOAA/PMEL's VENTS Program objectives in the area of assessing the effect of spreading-center hydrothermal vents on the marine environment and defining the tectonic and volcanological processes producing oceanic crust at the Juan de Fuca Ridge. The research that CIMRS is involved with in NOAA's VENTS Program falls into three main areas: photogeologic characterization of seafloor; acoustic imaging and interpretation of the seafloor; and T-phase event detection. Specifically, studies include the interpretation of geologic structure via seafloor remote-sensing techniques, determining seafloor physical properties from acoustic backscatter data, and the understanding of plate boundary mechanics from acoustical/seismological investigations.

Four CIMRS research assistants and two research associates contribute directly to the VENTS Program in various components of computer support and scientific research on the Juan de Fuca Ridge. A very important and time-consuming project completed this year was the refinement and improvement of processing methods used on navigation data from towed camera sled and *Alvin* submersible operations. This project necessitated the development of five new software programs to be used specifically for this navigational data. The software developed was then used to reprocess data gathered on the Juan de Fuca Ridge from 1986–1989 and create a compatible year-to-year data base by converting all camera and submersible navigation data to a Universal Transverse Mercator grid. Similarly, software was developed for sidescan sonar image enhancement of the seafloor. A new program was written to correct navigated sidescan images based on bathymetric data by adjusting the position of the navigated sidescan image to match the seafloor terrain more closely, thus reducing distortion of the image. Previously developed software for interpreting photogeologic data was modified this year to use latitude and longitude as mapping coordinates so that the plots generated from this data can match bathymetric maps of the same area. Additionally, two new programs were developed for this data to display microbathymetry along camera tow tracks in map view and in cross-section to aid in the geological interpretation of the seafloor.

An ongoing project is the improvement of computer software for processing raw Sea Beam backscatter data. The multi-beam echo-sounder Sea Beam is typically used for mapping the bathymetry of the deep-sea floor. However, additional information about the roughness properties of the seafloor can be extracted from the structure of the returned acoustic signal. This year a Kirchhoff-based model was applied to recorded acoustic backscatter data and preliminary results indicate that the model will provide more accurate descriptions of seafloor roughness parameters.

A new project begun in FY 90 is the development of T-phase event detection for the Juan de Fuca Ridge. During the 1989 VENTS cruise on the NOAA ship *Discoverer*, a successful test of

the existing hydrophones in the Pacific determined that these hydrophones can be used to detect acoustic tectonic and/or volcanic events along the ridge. If the technique proves to be successful for monitoring and locating submarine events, CIMRS research assistants will assist in a fast-response effort using shipboard instruments. During FY 91 CIMRS research assistants and associates will be developing computer programs to discriminate, analyze and locate T-phase events.

Accomplishments FY 90

- Developed an interactive editing/plotting computer program for processing all navigation data for VENTS project. Navigation data base now exists for Juan de Fuca Ridge from 1986–1989 for towed camera data.

- Technical reference manual written for documentation of processing sidescan data to generate navigated sidescan images of seafloor.

- Developed two computer programs to merge navigation data and sidescan field data in different formats. Data from 1985–1989 now merged can be used to produce navigated sidescan image maps.

- Completed analysis of 20,000 seafloor photographs from 1989 VENTS cruise, incorporated them into computer data base, and compiled photogeologic maps of the seafloor along the northern Cleft Segment of the Juan de Fuca Ridge.

- Developed two new plotting programs to display microbathymetric data together with photogeologic data from deep-sea camera surveys.

- Completed analysis of teleseismically recorded earthquakes along the Blanco Transform Fault Zone. Analysis established the relationship between the length of a strike-slip fault and the corresponding size of an earthquake, observed along continental strike-slip faults, for an oceanic transform.

- Created a data base of epicentral locations of teleseismically recorded earthquakes with particularly thorough coverage of the Juan de Fuca Ridge.

- Established a T-phase location data base from data collected at the Hawaii Institute of Geophysics not previously available on computer.

- Integrated gravity and magnetic surveys and Sea Beam data from the Juan de Fuca Ridge into models of crustal evolution.

- Presented three poster sessions at American Geophysical Union Conference by CIMRS researchers:

  "A Sea Beam, Gravity, and Magnetic Study of the Atlantic Transport at 30°N on the Mid-Atlantic Ridge"

"Is the Southern Juan de Fuca Ridge Undergoing an Episode of Seafloor Spreading?"

"Application of the Kirchhoff Approximation to Sea Beam Acoustic Returns"

Plans FY 91

- Develop models and signal processing software for analysis, detection and location of T-phase events along the Juan de Fuca Ridge.

- Develop design of, and submit proposal to fund, a new seafloor instrument array to monitor volcanic intrusions on Juan de Fuca ridge crest to test hypothesis that megaplumes are caused by seafloor spreading events.

- Continue to refine Kirchhoff approximation of Sea Beam backscatter data to determine the physical characteristics of the seafloor using the echo strength of the acoustic beam.

- Complete Sea Beam bathymetric data base of Juan de Fuca Ridge, compile into user friendly format for chart generation, create digital data base, and user's guide.

- Continue analysis of photogeologic and microbathymetry data of seafloor from camera tows during FY 90 field season, particularly the northern Cleft Segment of the Juan de Fuca Ridge.

- Develop and submit proposal to NSF for repeat Sea Beam surveys on the northern East Pacific Rise to detect recent volcanic eruptions on another ridge with higher spreading rates than the Juan de Fuca.

PMEL STAFF

OFFICE OF THE DIRECTOR

Eddie N. Bernard, Director
James R. Holbrook, Deputy Director
CAPT Michael A. McCallister, Associate Director

Bernard, Eddie N.	Director
Cahoon, Lenora J.	Secretary (Typing)
Cassady, Jeanne*	Secretary (Typing)
Holbrook, James R.	Supervisory Oceanographer
Jackson, Terry D., LCDR*	NOAA Corps
Kranz, Susan L.	Secretary (Typing)
McCallister, Michael A., CAPT	NOAA Corps

TECHNICAL AND ADMINISTRATIVE SUPPORT

Cynthia L. Loitsch, Program Support Officer

Anderson, James W.	Photographer
Angkico, Susana L.	Computer Programmer
Collins, Beverly J.	Budget Assistant
Conlan, Karen L.	Illustrator
Cooke, Florence K.	Travel Clerk
Curl, Virginia M.*	Illustrator
Elkins, Gayle L.	Motor Vehicle Operator
Loitsch, Cynthia L.	Program Support Manager
McLean, Allison*	Computer Assistant
O'Connor, Mark L.	Motor Vehicle Operator
Perry, Richard M.*	Motor Vehicle Operator
Smith, Claudia J.	Photographer
Snyder, Susan D.	Program Support Assistant
Thomasson, Norma H.	Support Services Supervisor
Vose, Virginia W.	Computer Clerk
Whitney, Ryan L.	Computer Operator

COMPUTER AND NETWORK SUPPORT

Paul Lu, Division Leader

Barzel, Ronald*	Communications Specialist
Bathurst, William	Computer Programmer

* No longer affiliated with PMEL

Beard, Emily, LTJG*	NOAA Corps
Borg-Breen, David	Computer Systems Programmer
Halsey, Timothy S., LTJG	NOAA Corps
Lu, Paul	Computer Specialist
McCarty, Laura C.	Computer Programmer
McGlothlen, Kenneth*	Computer Assistant
O'Brien, Julie A.	Lead Computer Operator
Renton, Mark*	JISAO/Research Scientist
Richards, Russell L.	Computer Equipment Analyst
Stewart, Christina	Computer Operator
Tanigawa, Dale*	Computer Operator
Vance, Tiffany C.	Computer Programmer
Walker, Andrew D.*	Computer Operator

ENGINEERING DEVELOPMENT DIVISION

Hugh B. Milburn, Division Leader

Delizo, Stan W.*	Engineering Technician
Gable, James R.	Electronics Technician
Holzer, Dennis E.	Instrument Maker
Jackson, Thomas G.	Electronics Technician
Johnson, James M.	JISAO/Marine Technician
Kinsey, Kevin	Laborer Technician
Mader, Floyd W.	Electronics Technician
McLain, Patrick D.	Electronics Engineer
Meinig, Christian, LTJG	NOAA Corps
Milburn, Hugh B.	Supervisory General Engineer
Miller, Hendrick	Engineering Technician
Nakamura, Alex I.	Electronics Engineer
Newman, Roy	Electronics Technician
Schattgen, Paul L., LTJG*	NOAA Corps
Shanley, John C.	Engineering Aid
Stapp, Michael F.	Electronics Technician

MARINE ASSESSMENT RESEARCH DIVISION

Herbert C. Curl, Jr., Division Leader

Cannon, Glenn A.	Oceanographer
Cokelet, Edward D.	Oceanographer
Cudaback, Cynthia N., LTJG	NOAA Corps
Curl, Herbert C., Jr.	Supervisory Oceanographer
Hamilton, Sharon	Physical Science Technician

* No longer affiliated with PMEL

Herzog, Carolyn	Secretary
Lavelle, John W.	Oceanographer
Mofjeld, Harold O.	Oceanographer
Pashinski, David J.	Oceanographer
Paulson, Anthony J.	Oceanographer

MARINE RESOURCES RESEARCH DIVISION

Stephen R. Hammond, Division Leader

Appelgate, Bruce	CIMRS/Research Assistant
Baker, Edward T.	Oceanographer
Chadwick, William W.	CIMRS/Research Assistant
Clapp, Daniel L.	CIMRS/Research Assistant
Dziak, Robert P.	CIMRS/Research Assistant
Embley, Robert W.	Geophysicist
Feely, Richard A.	Oceanographer
Fox, Christopher G.	Physical Scientist
Geiselman, Terri L.*	Oceanographer
Gendron, James F.	Chemist
Hammond, Stephen R.	Supervisory Oceanographer
Hillard, Bruce F., LCDR	NOAA Corps
Jones, Frederick J., CDR*	NOAA Corps
Lau, Andy	CIMRS/Research Assistant
Lebon, Geoffrey	JISAO/Research Scientist
Lemon, Michael, LTJG	NOAA Corps
Massoth, Gary J.	Oceanographer
Matsuura, Hiroshi	JISAO/Research Assistant
Meis, Philip J., LTJG	NOAA Corps
Nitchman, Catherine, LTJG	NOAA Corps
Restrepo, Maria J.	CIMRS/Research Assistant
Roberts, Marilyn F.	Physical Science Technician
Roe, Kevin K.	JISAO/Research Scientist
Seem, Dennis, LT	NOAA Corps
Tennant, David A.	Oceanographer
Waddell, Jessica L.	CIMRS/Administrative Assistant
Walker, Sharon L.	Oceanographer
Zervas, Christopher	CIMRS/Research Assistant

* No longer affiliated with PMEL

MARINE SERVICES RESEARCH DIVISION

James E. Overland, Division Leader

Aagaard, Knut	Oceanographer
Berggren, Todd, LTJG	NOAA Corps
Blake, Wade J., LTJG*	NOAA Corps
Bond, Nicholas	JISAO/Postdoctorate
Creswell, W. Austin, LTJG	NOAA Corps
Darnall, Clark	JISAO/Research Engineer
DeWitt, Carol L.	Physical Science Technician
Dougherty, Daniel	Physical Science Technician
Eble, Marie	Oceanographer
Gonzalez, Frank I.	Oceanographer
Gray, Judith G.*	Meteorologist
Kachel, David G.	Computer Programmer
Lawrence, Leslie	Physical Scientist
Long, Virginia L.	Physical Science Technician
Macklin, Stewart A.	Meteorologist
Overland, James E.	Supervisory Oceanographer
Parker, William J.	Field Operations Specialist
Pease, Carol H.	Oceanographer
Proctor, Peter D.*	Physical Science Aid
Reed, Ronald K.	Oceanographer
Roach, Andrew T.	Oceanographer
Salo, Sigrid A.	Oceanographer
Schall, Marie L.	Physical Science Technician
Schumacher, James D.	Oceanographer
Spillane, Michael	JISAO/Research Scientist
Stabeno, Phyllis J.	Oceanographer
Turet, Philip	JISAO/Research Scientist
Wilson-Boyd, Belle	Editorial Assistant

OCEAN CLIMATE RESEARCH DIVISION

Stanley P. Hayes, Division Leader

Bates, Timothy S.	Research Chemist
Benson, Jeffrey B.	Physical Science Technician
Brainard, Russell E., LT	NOAA Corps
Bullister, John L.	Oceanographer
Calhoun, Julie	JISAO/Graduate Research Assistant
Cass, Vallapha	Secretary
Chang, Ping*	JISAO/Postdoctorate
Coho, Carolyn S., ENS*	NOAA Corps

* No longer affiliated with PMEL

Cosca, Cathy	JISAO/Scientific Programmer
Craig, Anthony	UW/Graduate Student
Davison, Jerry C.	JISAO/Research Scientist
Freitag, Howard P.	Oceanographer
Gifford, Sue E.	Secretary (Typing)
Hankin, Steven	Computer Programmer
Harrison, Don E.	Oceanographer
Hayes, Stanley P.	Supervisory Oceanographer
Johnson, Eric	NRC Postdoctorate
Johnson, James E.	JISAO/Research Scientist
Kelly, Kimberly C.	Oceanographer
Kuroda, Yoshifumi	Visiting Scientist (Japan)
Larsen, Jimmy C.	Oceanographer
Leck, Caroline	Visiting Scientist (Sweden)
Lee, Daniel	JISAO/Scientific Programmer
LoConte, John L.	Electronics Technician
Mangum, Linda J.	Oceanographer
Manke, Ansley B.	Computer Programmer
McCarty, Marguerite	JISAO/Research Scientist
McClurg, Dai	Computer Programmer
McPhaden, Michael J.	Oceanographer
McTaggart, Kristine	JISAO/Physical Science Technician
Menzia, Fred	JISAO/Research Scientist
Moore, Ben A.	Electronics Technician
Murphy, Paulette P.	Chemist
Neander, Julia N., LTJG	NOAA Corps
O'Brien, Kevin	Computer Assistant
Pullen, Patricia E.	Oceanographer
Quinn, Patricia	CIRES/Postdoctorate
Rogers, Paul	UW/Graduate Student
Root, David L.	Laborer
Roupe, Kelly*	Physical Science Technician
Shepherd, Andrew J.	Field Operations Specialist
Soreide, Nancy N.	Computer Programmer
Steffin, Otto F., CAPT	NOAA Corps (on loan from NOS)
Stratton, Linda	JISAO/Scientific Programmer
Taft, Bruce A.	Oceanographer
Verschell, Mark A.*	JISAO/Scientific Programmer
Wilson, Clifford C., LTJG*	NOAA Corps
Wisegarver, David P.	Chemist
Wolfe, Gordon	JISAO/Graduate Research Assistant
Zimmerman, David K., LT	NOAA Corps

* No longer affiliated with PMEL

PMEL SEMINARS

Dates	*Name and Affiliation*	*Seminar Topic*
1989		
19 October	Dr. Trevor McDougall CSIRO Division of Oceanography Hobart, Tasmania Australia	Vertical mixing in ocean circulation
26 October	Dr. Douglas Wallace Brookhaven National Laboratory Upton, New York	Transient tracer water mass dating
16 November	Dr. Barbara Hickey School of Oceanography University of Washington	Circulation off the Washington coast: whence and whither
14 December	Dr. Stephen Riser School of Oceanography University of Washington	North Pacific Intermediate Water production
1990		
8 February	Dr. James W. Murray School of Oceanography University of Washington	Global ocean flux studies in the Equatorial Pacific
1 February	Dr. John M. Wallace Department of Atmospheric Sciences University of Washington	Meteorological aspects of ENSO
27 February	Dr. George Philander NOAA/GFDL Geophysical Fluid Dynamics Laboratory Princeton University Princeton, NJ	ENSO families

22 March	Dr. John Lupton Department of Marine Sciences University of California at Santa Barbara	Mapping the hydrothermal effluent from the Juan de Fuca Ridge using ^3He
8 March	Dr. Joel Picaut ORSTOM New Caledonia	Equatorial Kelvin and Rossby waves in the Pacific During El Niño 1986–87 using Geosat sea level and derived surface currents
29 March	Mr. Gregory Johnson Woods Hole Oceanographic Institution Woods Hole, MA	Circulation of bottom water in the Somali Basin
5 April	Dr. Mark A. Johnson Mesoscale Air-Sea Interaction Group Florida State University Tallahassee, FL	The northeast Pacific Ocean response
9 April	Mr. Avijit Gangopadhyay University of Rhode Island Narragansett, RI	Wind-forcing of the Gulf Stream
13 April	Dr. Robbie Toggweiler NOAA/GFDL Princeton University Princeton, NJ	On the origin of the upwelled low-C_{14} surface water in the eastern equatorial Pacific
17 May	Dr. Richard E. Thomson Institute of Ocean Sciences Sidney, B.C., Canada	Lagrangian subsurface currents in the northeast Pacific: Eddy and dispersion characteristics
1 June	Syd Levitus NOAA/GFDL Princeton University Princeton, NJ	Temporal variability in the thermohaline structure of the north Atlantic
26 April	Dr. Al Hermann Woods Hole Oceanographic Institution Woods Hole, MA	Modeling the geostrophic adjustment and spreading of water formed by deep convection
3 May	Michael Spillane Tetra Tech Inc. Bellevue, WA	On intraseasonal oscillation in sea level along the west coast of the Americas

21 June	Torgny Vinje Norwegian Polar Research Institute Oslo, Norway	Exchange of sea ice in the European sector of the Arctic
28 June	Nancy Soreide Ocean Climate Research Division NOAA/PMEL	EPIC...A system for management, analysis and display of oceanographic time-series and hydrographic data
5 July	Judy Gray Marine Services Research Division NOAA/PMEL	A focus on FOCI: The last will and testament of Judy Gray
6 September	J. William Lavelle Marine Assessment Research Division NOAA/PMEL	A model study of density intrusions into, and circulation within, Puget Sound
10 September	Trond Aukrust IBM Bergen Scientific Centre Bergen High Technology Centre Bergen, Norway	Numerical simulation of the 3-D circulation in the North Atlantic, and the Norwegian, Greenland, and Barents Seas
18 September	Captain William L. Stubblefield NOAA Office of the Chief Scientist Silver Spring, MD	NOAA Fleet Modernization Study: Phase I & II:
20 September	Eric D'Asaro Applied Physics Laboratory University of Washington	Small-scale mixing and the heat budget of the Arctic Ocean

JISAO SEMINARS

Dates	*Name and Affiliation*	*Seminar Topic*
1989		
17 October	Dr. Francisco Chavez Monterey Bay Aquariam Research Institute Pacific Grove, CA	Primary productivity in the equatorial Pacific Ocean
23 October	Dr. Ute Luksch Max Planck Institüt für Meteorologie Hamburg, Federal Republic of Germany	Simulations of the interannual sea surface temperature variability in the North Pacific
6 November	Dr. Richard Seager Atmospheric and Planetary Science Columbia University Palisades, NY	Modeling tropical Pacific sea surface temperature (SST)
7 November	"	A simple model of the climatology of the low-wind field in the Tropics
15 November	Dr. Richard Dugdale Allan Hancock Foundation University of Southern California	New productivity in the central equatorial Pacific
21 November	Dr. Thomas Braziunas Department of Geological Science University of Washington	Carbon ^{14}C as a tracer of holocene variations in atmosphere/ocean CO_2 exchange and oceanic vertical mixing
4 December	Dr. Eugene M. Rasmusson University of Maryland College Park, MA	Biennial component of ENSO

1990

9 January	Dr. Hiroshi Kanzawa National Institute of Polar Research Tokyo, Japan	Observation of ozone and related quantities by Japanese Antarctic Research Expedition with emphasis on a planned Polar Patrol Balloon (PPB) project
17 January	Dr. Marlon Lewis NASA Headquarters Dalhousie University Halifax, Nova Scotia	Equatorial fluxes of heat nitrate and carbon
22 January	Dr. Anthony Moura National Institute for Space Studies Dos Campos, Brazil	The international TOGA program
8 February	Dr. Hideharu Akiyoshi Kyushu University Japan	The global and seasonal variation of ozone simulated by a simple two-dimensional model
12 February	Dr. Mojib Latif Max Planck Institüt für Meteorologie Hamburg, Federal Republic of Germany	Predictability of an ocean general circulation model with empirical atmospheric feedback
12 February	Dr. David Battisti Department of Meteorology University of Wisconsin Madison, WI	Modeling the tropical atmosphere circulation with an eye towards coupled atmosphere-ocean interaction
28 February	Dr. Bin Wang Meteorology Department University of Hawaii Honolulu, HI	Dynamics of tropical intraseasonal convection anomalies: observations and theory
1 March	Dr. George Philander Princeton University Princeton, NJ	Air-sea interaction and climate changes caused by precession of the equinoxes
8 March	Dr. Hiroshi Kawamura Department of Geophysics Tohoku University Japan	Turbulence structures above and below wind waves

17 April	Dr. Edwin K. Schneider Center for Ocean-Land-Atmosphere Interactions University of Maryland College Park, MA	Hadley circulation
25 April	Dr. Pat Wheeler College of Oceanography Oregon State University Corvallis, OR	Biological factors affecting NO_3 use by marine phytoplankton
2 May	Dr. Mark Altabet Department of Chemistry Woods Hole Oceanographic Institution Woods Hole, MA	Use of nitrogen isotopes to study processes in the marine environment
3 May	Dr. Yoshi Wakata Tokai University Japan	The ENSO cycle viewed in terms of a switching mechanism
23 May	Dr. David Lea Department of Geology University of California Santa Barbara, CA	Barium as a paleoceanographic tracer
6 August	Dr. Kasimir Kondratovich Department of Dynamic Atmosphere and Space Research of the Earth Hydrometeorological Institute Leningrad, USSR	Recent climatic change and its relation to the westward drift of the magnetic field and ozonosphere
17 September	Dr. Masahide Kimoto Department of Atmospheric Sciences University of California Los Angeles, CA	Multiple flow regimes in the northern hemisphere winter

JIMAR SEMINARS

Dates	*Name and Affiliation*	*Seminar Topic*
1989		
3 November	William W. Kellogg National Center for Atmospheric Research Boulder, CO	Climate modeling and climate change
21 December	Dr. John McCarthy Research Applications Program National Center for Atmospheric Research Boulder, CO	An integrated terminal weather hazard detection and warning system: recent operational experiences at Denver with a prototype wind shear Doppler Radar system
1990		
16 March	Dr. Mark Cane Lamont-Doherty Geological Observatory Columbia University Palisades, NY	Seminar, map reading, guruspeak and informal (off the record) discussion on prediction, detection, and diagnosis of El Niño.
19 March	"	Is this the mechanism of El Niño and the Southern Oscillation?
16 April	Dr. Igor Mokhov Department of Atmospheric Sciences University of Illinois at Urbana Urbana, IL	Some results on analysis of global climate field evolution in the annual cycle and interannual variability
17 May	Dr. Steven Lyons Department of Meteorology Texas A&M University College Station, TX	Origins of convective variability over equatorial southern Africa during austral summer
5 July	Dr. Gary Barnes National Center for Atmospheric Research Boulder, CO	A convective cell in a hurricane rainband

2 August	Dr. Friedrich Schott Institüt für Meereskunde Kiel, Federal Republic of Germany	Direct current measurements in winter convection regimes: Mediterranean and Greenland Sea

PMEL PUBLICATIONS

AAGAARD, K., and E.C. Carmack. The role of sea ice and other fresh water in the arctic circulation. *Journal of Geophysical Research, 94*(C10), 14,485–14,498 (1989).

Salinity stratification is critical to the vertical circulation of the high-latitude ocean. We here examine the control of the vertical circulation in the northern seas, and the potential for altering it, by considering the budgets and storage of fresh water in the Arctic Ocean and in the convective regions to the south. We find that the present-day Greenland and Iceland seas, and probably also the Labrador Sea, are rather delicately poised with respect to their ability to sustain convection. Small variations in the fresh water supplied to the convective gyres from the Arctic Ocean via the East Greenland Current can alter or stop the convection in what may be a modern analog to the halocline catastrophes proposed for the distant past. The North Atlantic salinity anomaly of the 1960s and 1970s is a recent example; it must have had its origin in an increased fresh water discharge from the Arctic Ocean. Similarly, the freshening and cooling of the deep North Atlantic in recent years is a likely manifestation of the increased transfer of fresh water from the Arctic Ocean into the convective gyres. Finally, we note that because of the temperature dependence of compressibility, a slight salinity stratification in the convective gyres is required to efficiently ventilate the deep ocean.

AAGAARD, K., C.H. PEASE, A.T. ROACH, and S.A. SALO. Beaufort Sea mesoscale circulation study—Final Report. NOAA TM ERL PMEL-90 (NTIS PB90-158775), 114 pp. (1989).

The Beaufort Sea Mesoscale Project was undertaken to provide a quantitative understanding of the circulation over the Beaufort Sea shelf and of its atmospheric and oceanic forcing. Major emphasis has been placed on providing extensive synoptic oceanographic and meteorological coverage of the Alaskan Beaufort Sea during 1986–88. In addition, supplementary measurements have been made in the southern upstream waters of Bering Strait and the Chukchi Sea. The work has resulted in an unprecedented regional data set for both the ocean and the atmosphere. The principal conclusions are as follows: 1) Below the upper 40–50 m of the ocean, the major circulation feature of the outer shelf and slope is the Beaufort Undercurrent, a strong flow which is directed eastward in the mean, but which is subject to frequent reversals toward the west. The reversals are normally associated with upwelling onto the outer shelf. The undercurrent is very likely part of a basin-scale circulation within the Arctic Ocean. 2) While we find statistically significant wind influence on the subsurface flow in the southern Beaufort Sea, it is generally of secondary importance, accounting for less than 25% of the flow variance below 60 m. An important implication is that at least below the mixed layer, the circulation on the relatively narrow Beaufort shelf is primarily forced by the ocean rather than by the local wind. This oceanic forcing includes shelf waves and eddies. Therefore, to the extent that a localized problem or process study requires consideration of the shelf circulation, such as would be the case for oil-spill trajectory modeling, a larger-scale framework must be provided, within which the more local problem may be nested. 3) There were large changes in wind variance with season, with the largest variances occurring in the late summer/early autumn and again in January because of

blocking ridges in the North Pacific shifting the storm track westward over the west coast of Alaska and across the North Slope. 4) Despite the seasonally varying wind field, as well as the large seasonal differences in the upper-ocean temperature and salinity fields, we find no evidence for a seasonal variability in the subsurface circulation in the Beaufort Sea. This situation contrasts with that in Bering Strait and probably in the Chukchi Sea, where a seasonal cycle in the transport is apparent. Therefore, while the northward flow of water from the Pacific is of major significance to the structure and chemistry of the upper ocean in the Arctic (including the Beaufort Sea), as well as its ice cover and biota, the dynamic significance of that flow to the Beaufort Sea appears small. 5) In contrast to the lack of a seasonal oceanographic signal at depth, the interannual variability in the flow characteristics can be considerable. For example, during the period fall 1986-spring 1987, the Beaufort Undercurrent appears to have been deeper by 30–40 m compared with both earlier and ensuing measurements. The consequences of such anomalies for the upper-ocean velocity structure and transport are likely significant. 6) During much of the experiment, the meteorological conditions were milder than normal, consistent with less coastal ice in the summer and autumn, the passage of more storms up the west coast of Alaska and across the North Slope, and generally higher air temperatures along the North Slope. These climatological near-minimum ice years were followed in 1988 by the heaviest summer ice along the Chukchi coast since 1975. 7) The atmospheric sea-level pressure field was well represented by the METLIB products from the FNOC surface analysis if the 12-hour lag of the FNOC pressures was taken into account. However, the FNOC surface air temperature field does not accurately represent either the land-based stations or the drifting ice buoys. The errors in the FNOC temperature field showed a systematic over-prediction during winter and spring of 10–20°C, leading to an annual over-prediction of air temperature by 3–13°C at all sites. Gradient winds from FNOC are therefore well suited for modeling purposes if they are calculated from the time-shifted surface analysis, but the FNOC surface temperature analysis should not be used for any model calculations, except perhaps as an upper boundary condition for a rather complete planetary boundary layer model.

Appelgate, T.B., Jr. Volcanic and structural morphology of the south flank of Axial Volcano, Juan de Fuca Ridge: Results from a Sea MARC I side scan sonar survey. *Journal of Geophysical Research, 95*(B8), 12,765–12,783 (1990).

A 1500 km^2 Sea MARC I side scan sonar survey south of Axial Volcano investigated the geological structure and constitution of the South Axial Rift Zone (SARZ) and the northern 30 km of the Vance spreading segment. Relative age assignments based on structural relationships indicate that recent volcanism on the southern flank of Axial Volcano has been restricted to the SARZ. The surficial volcanic morphology of the SARZ changes downrift, from linear volcanic ridges (north) to small (1-km diameter) cratered cones (south), perhaps indicating a variation in eruptive vent geometry from fissures to point sources downrift. Recent lavas on the northern and central SARZ erupted along preexisting faults in the underlying crust. By acting as pathways for SARZ magmas, these faults may have controlled the orientation of SARZ volcanic ridges and perhaps the orientation of the entire SARZ edifice. The Vance spreading segment terminates at 45°40'N and is not linked with a transform fault. The axis of spreading between 45°40'N and 46°00'N is offset west of the Vance segment and is constrained to lie between 129°54'W and 130°06'W. A discrete,

structurally defined spreading axis, however, is not evident over the southern flank of Axial Volcano. The divergent plate boundary may now underlie the SARZ massif, although South Helium Basin (an embayment in the southeast flank of Axial Volcano) has undergone, and may continue to accommodate, crustal extension. A 48 km^2 lava field discovered east of the SARZ is composed of lavas that are inferred to have erupted from the SARZ. These lavas can be traced eastward from the SARZ into the axial valley of the northern Vance segment and partially fill the valley with lavas up to 60 m thick. The eruption of these lavas, which occupy an estimated volume of 1.8 km^3, may have contributed to the formation of Axial Volcano's summit caldera.

Arlander, D.W., D.R. Cronn, J.C. Farmer, F.A. Menzia, and H.H. Westberg. Gaseous oxygenated hydrocarbons in the remote marine troposphere. *Journal of Geophysical Research, 95*(D10), 16,391–16,403 (1990).

Measurement of the background levels and study of the chemistry of trace organic carbon species in the remote marine troposphere occurred during an April–July 1987 SAGA II cruise in remote regions of the Pacific and Indian Oceans. Measured compounds included carboxylic acids, formaldehyde, light hydrocarbons (C_2–C_4), and ozone. The results show seasonal, diel, and spatial dependencies for the organic acids. Distinct latitudinal gradients are seen for most sampled compounds. Formic acid is well correlated with suspected precursors, formaldehyde and light hydrocarbons. Acetic acid follows a similar pattern as formic acid, although its precursors are as yet undefined. Diel patterns of low amplitude for the organic acids in the remote marine troposphere suggest a natural contribution to tropospheric photochemistry, and to the global carbon cycle as well. For the northern hemisphere Pacific Ocean, the mean formic acid mixing ratio was 0.80 ± 0.30 ppbv, the mean acetic acid value was 0.78 ± 0.32 ppbv. For the southern hemisphere Pacific Ocean, formic acid averaged 0.22 ± 0.13 ppbv, for acetic acid, the mean was 0.28 ± 0.17 ppbv. For the northern hemisphere Indian Ocean, the mean formic acid mixing ratio was 0.75 ± 0.24 ppbv, and the mean acetic acid value was 0.69 ± 0.27 ppbv. For the southern hemisphere Indian Ocean, the mean formic acid value was 0.19 ± 0.18 ppbv, and the mean acetic acid value was 0.29 ± 0.16 ppbv. Highest levels of organic acids were encountered near known anthropogenic source regions, in air masses of continental origin, or near regions of naturally produced alkenes (C_2, C_3). The ozone-alkene oxidation scheme appears to play a major role in gas phase organic acid production in the remote marine troposphere. Nighttime gas phase deposition of the organic acids onto the ocean surface appears to be a major sink.

BAKER, E.T. Hydrothermal plume prospecting: hydrographic and geochemical techniques. In *Gorda Ridge: A Seafloor Spreading Center in the United States Exclusive Economic Zone*, G.R. McMurray (ed.). Springer-Verlag, New York, 155–167 (1990).

Hydrothermal plumes, formed by the mixing of hot vent fluids and ambient seawater, can be used to locate, characterize, and quantify sources of seafloor hydrothermal emissions. Vent fluids typically undergo a 10^4-fold dilution as they rise several hundred meters above the sea floor and form neutrally buoyant plumes with heat and chemical anomalies that stretch tens to thousands of kilometers downcurrent of their source. Real-time mapping of

these plumes by towing sensitive hydrographic and optical sensors from a surface ship can efficiently locate the plume source, guide discrete chemical sampling of the diluted hydrothermal fluids, and estimate the heat and mass flux of individual vent fields. This paper uses case histories of investigations along the Juan de Fuca and Gorda Ridges to describe strategies for mapping and characterizing hydrothermal plumes at spatial scales ranging from hundreds of meters to hundreds of kilometers.

BAKER, E.T., and J.E. Lupton. Changes in submarine hydrothermal ^{3}He/heat ratios as an indicator of magmatic/tectonic activity. *Nature, 346,* 556–558 (1990).

An important question in submarine hydrothermal research concerns the connection between hydrothermal discharge from a spreading centre and variations in local magmatic and tectonic activity. Because it is likely that tectonic stretching and concomitant shallow magmatic activity triggered the cataclysmic venting that created the Juan de Fuca Ridge "megaplumes," we have for three years monitored the ^{3}He concentration and temperature anomaly of the underlying steady-state plume at the site of the original megaplume. We report here that the apparent ^{3}He/heat ratio in the steady-state plume has progressively decreased from 4.4 to 2.4 to 1.3×10^{-12} cm^3 STP cal^{-1}, changing from a uniquely high ratio to one characteristic of established vent fields on other ridge segments. We propose that the initially high ^{3}He/heat ratio, sampled within days of the megaplume eruption, resulted from magma degassing into a hydrothermal circulation system of high permeability and short fluid residence time. Thus, high ^{3}He/heat ratios may indicate venting created or profoundly perturbed by a magmatic-tectonic event, and lower ratios may typify systems at equilibrium.

BAKER, E.T., R.E. McDuff, and G.J. MASSOTH. Hydrothermal venting from the summit of a ridge axis seamount: Axial Volcano, Juan de Fuca Ridge. *Journal of Geophysical Research, 95*(B8), 12,843–12,854 (1990).

We have mapped the distribution and intensity of submarine hydrothermal emissions from the summit caldera of Axial Volcano by means of hydrographic and chemical sampling of the water column during annual cruises in four consecutive years (1985–1988). These investigations were undertaken to ascertain the strength of hydrothermal venting relative to other vent fields on the Juan de Fuca Ridge and to gauge the importance of Axial Volcano as a source of hydrothermal emissions to the northeast Pacific Ocean. Measurable temperature anomalies are mostly restricted to a 200-m-thick water column within the caldera, where they range from a background level of ~0.01°C to local maxima of 0.02–0.1°C above known high-temperature vent fields. The temperature anomaly plume is significantly smaller in both extent and intensity than plumes emitted by vent fields on other segments of the Juan de Fuca Ridge. A maximum estimate of the total heat flux from the summit, based on the total excess heat and advective velocity of the plume, is 8×10^8 W. Hydrothermal venting seems surprisingly small for an edifice that testifies to a long-term oversupply of magma at a single axial location. We speculate that additional heat may be lost from Axial Volcano by diffuse percolation of seawater over broad areas of its flanks and by magma eruption and venting along flank rift zones.

Bane, J.M., C.D. Winant, and J.E. OVERLAND. Planning for coastal air-sea interaction studies in CoPO. *Bulletin of the American Meteorological Society, 71*(4), 514–519 (1990).

A number of observational programs have been carried out on the United States continental shelf to describe coastal-ocean circulation with emphasis on mesoscale processes. In several of these studies the atmosphere was found to play a central role in determining the coastal circulation through either local or remote forcing. Because of these results, the Coastal Physical Oceanography (CoPO) planning effort has designated three coastal air-sea interaction areas to focus on in a national program to study the physical processes on the continental shelf. These areas are shelf frontogenesis, interaction of stable layers with topography, and forcing by severe storms. The long-term objective of the air-sea interaction component of CoPO is to better understand the structure, dynamics, and evolution of the various mesoscale and synoptic-scale processes that significantly affect coastal/shelf circulation through air-sea interactions. Within this body of knowledge will be an improved quantification of the air-sea exchanges of dynamically important quantities set in the framework of mesoscale and synoptic-scale processes.

BATES, T.S., A.D. Clarke, V.N. Kapustin, J.E. Johnson, and R.J. Charlson. Oceanic dimethylsulfide and marine aerosol: Difficulties associated with assessing their covariance. *Global Biogeochemical Cycles, 3*(4), 299–304 (1989).

Simultaneous measurements of oceanic dimethylsulfide (DMS), atmospheric aerosol sulfate and the size-resolved physical properties of the aerosol were made aboard a ship in the equatorial Pacific during July 1987. Under light and variable winds, in an area essentially free of continental and anthropogenic air masses, an observed increase in oceanic DMS concentrations preceded simultaneous increases in non-sea salt sulfate aerosol, the fraction of volatile submicrometer (sub-μm) aerosol, the condensation nuclei population, and the mean particle diameter of the sub-μm aerosol. Although the increase in oceanic DMS can qualitatively account for the corresponding changes in the atmospheric aerosol particles, there are numerous difficulties in quantifying the relationship between the sea-to-air flux of DMS and the formation and growth of atmospheric aerosol particles.

BATES, T.S., J.E. JOHNSON, P.K. Quinn, P.D. GOLDAN, W.C. KUSTER, D.C. Covert, and C.J. Hahn. The biogeochemical sulfur cycle in the marine boundary layer over the northeast Pacific Ocean. *Journal of Atmospheric Chemistry, 10*(1), 59–81 (1990).

The major components of the marine boundary layer biogeochemical sulfur cycle were measured simultaneously onshore and off the coast of Washington State, U.S.A. during May 1987. Seawater dimethylsulfide (DMS) concentrations on the continental shelf were strongly influenced by coastal upwelling. Concentrations further offshore were typical of summer values (2.2 nmol/L) at this latitude. Although seawater DMS concentrations were high on the biologically productive continental shelf (2–12 nmol/L), this region had no measurable effect on atmospheric DMS concentrations. Atmospheric DMS concentrations (0.1–12 nmol/m^3), however, were extremely dependent upon wind speed and boundary layer height. Although there appeared to be an appreciable input of non-sea-salt sulfate to the

marine boundary layer from the free troposphere, the local flux of DMS from the ocean to the atmosphere was sufficient to balance the remainder of the sulfur budget.

Bender, M.L., and M.J. MCPHADEN. Anomalous nutrient distribution in the equatorial Pacific in April 1988: evidence for rapid biological uptake. *Deep-Sea Research,* 37(7), 1075–1084 (1990).

Nutrients in the central equatorial Pacific are normally enriched at the Equator, with concentrations gradually falling to the north and south. This pattern reflects input by equatorial upwelling, with slow removal as waters flow poleward. In April 1988, we observed *minima* in SiO_2 and NO_{3-} + NO_{2-} concentrations near the Equator. [SiO_2] in particular dropped to minima at 2.5°N and 1–2.5°S, rose to maxima at 3°N and 3–6°S, then fell off in the normal pattern. Such minima are unusual features not clearly evident in data from other equatorial Pacific transects. A period of anomalous hydrographic conditions preceded the time of our chemical observations. Between February 1988 and April 1988, the anomalously warm conditions which characterized the equatorial Pacific during the 1986–1987 El Niño/Southern Oscillation event ended, and the thermocline shoaled sharply. We speculate that the anomalous nutrient distributions we observed in April are related to the regional hydrography of the preceding months. Physical forcing may have triggered rapid biological SiO_2 and NO_{3-} removal, producing the anomalous nutrient distribution we observed.

BERNARD, E.N., R.R. Behn, G.T. Hebenstreit, F.I. GONZALEZ, P. Krumpe, J.F. Lander, E. Lorca, P.M. McManamon, and H.B. MILBURN. On mitigating rapid onset natural disasters: Project THRUST (Tsunami Hazards Reduction Utilizing Systems Technology). Proceedings of Workshop XLVI, The 7th U.S.-Japan Seminar on Earthquake Prediction, Menlo Park, CA, 12–15 September 1988. USGS Open-File Report 90-98, 125–130 (1990).

Rapid onset natural hazards have claimed more than 2.8 million lives worldwide in the past 20 years. This category includes such events as earthquakes, landslides, hurricanes, tornados, floods, volcanic eruptions, wildfires, and tsunamis. Effective hazard mitigation is particularly difficult in such cases, since the time available to issue warnings can be very short or even nonexistent. This paper presents the concept of a local warning system that exploits and integrates the existing technologies of risk evaluation, environmental measurement, and telecommunications. We describe Project THRUST, a successful implementation of this general, systematic approach to tsunamis. The general approach includes pre-event emergency planning, real-time hazard assessment, and rapid warning via satellite communication links.

BERNARD, E.N., H.B. MILBURN, and T.D. JACKSON. Innovative Oceanography—Pacific Marine Environmental Laboratory's contributions to observing the oceans. Conference Record, The 16th Joint Meeting of the U.S.-Japan Cooperative Program in Natural Resources (UJNR) Marine Facilities Panel, Japan, September 1989, 473–478 (1989).

No abstract.

Busalacchi, A.J., M.J. MCPHADEN, J. Picaut, and S.R. Springer. Sensitivity of wind-driven tropical Pacific Ocean simulations on seasonal and interannual time scales. *Journal of Marine Systems, 1*, 119–154 (1990).

The purposes of this study are (1) to characterize differences in the time/space structure of various multiyear surface wind products for the tropical Pacific; and (2) to quantify the impact these differences may have on our ability to model oceanic wind-forced variability on seasonal and interannual time scales. Three coincident wind field analyses are used, viz. the Florida State University (FSU) subjective analysis, the University of Hawaii (SAWIN) subjective analysis and the Fleet Numerical Oceanography Center (FNOC) operational analysis. The five years chosen for study, 1979–1983, encompass three years of a fairly regular seasonal cycle leading up to the 1982–1983 El Niño. A linear multi-vertical model model is forced with these analyses; model dynamic height and sea level are then compared with observations based on expendable bathythermograph and island tide gauge data. The mean seasonal cycle prior to El Niño (1979–1981) is considered first, which then serves as a self-consistent basis for analyzing the interannual variability, particularly the significant anomalies about the mean in 1982–1983. The impact of discrepancies in the forcing functions is discussed relative to the dominant seasonal and interannual scales of variability for the wind-driven oceanic response. The analyses of the wind products and model solutions indicate the need for special attention to the wind stress curl fields when evaluating wind products for use in tropical oceanographic applications. On seasonal time scales, critical differences in the wind stress products, of order 0.2–0.4 dyn cm^{-2}, are in wind regimes of surface convergence and significant gradients such as the ITCZ and SPCZ. These uncertainties in the wind fields, or more appropriately the wind stress curl distributions, are manifested in model sea level solutions as 6–12 cm discrepancies near the NECC Trough and east of New Guinea. On average, the seasonal amplitude of the wind-forced sea level response in any one simulation is of the same order as the differences between any two sea level simulations. The interannual variability is dominated by the anomalies associated with the 1982–1983 El Niño. Root mean square differences between the product versus product wind stress anomalies range from 0.1–0.2 dyn cm^{-2} along the major ship tracks and up to 0.5 dyn cm^{-2} away from the shipping lanes. The basin-wide average of the rms differences, approximately 0.25 dyn cm^{-2}, is of similar magnitude to the average wind stress anomaly. Discrepancies in the interannual variability of the wind products lead to large-scale differences in the model sea level anomalies of up to 9–21 cm. The anomalous year to year variability of model sea level is of similar order in each of the simulations. Results for the FSU and SAWIN forced simulations are generally in better agreement with the observations than the FNOC simulation, especially during the 1982–1983 El Niño.

Busalacchi, A.J., M.J. MCPHADEN, J. Picaut, and S.R. Springer. Uncertainties in tropical Pacific Ocean simulations: The seasonal and interannual sea level response to three analyses of the surface wind field. Proceedings of the Western Pacific International Meeting and Workshop on TOGA COARE, Nouméa, New Caledonia, May 24–30, 1989. ORSTOM, 367–377 (1989).

The purpose of this study is to characterize differences in time/space structure present among conventional descriptions of the tropical Pacific surface wind field, and in turn, to quantify the impact of these differences on our ability to model the dominant wind-forced variability

of the tropical Pacific Ocean on seasonal and interannual time scales. A linear, multiple vertical mode ocean model is used as a transfer function to determine the influence of three distinct surface wind stress products for the period 1979–1983. This five-year period was chosen for study because it encompasses three years of a fairly regular seasonal cycle leading up to the 1982–83 El Niño for which there are several coincident oceanic and surface wind data sets. The three different wind analyses used are the Florida State University subjective analysis, the University of Hawaii subjective analysis, and the Fleet Numerical Oceanography Center objective analysis. We examine first the three mean seasonal cycle solutions prior to El Niño which then serve as self-consistent bases for analyzing the significant anomalies about the mean in 1982–83. The impact of uncertainties in the forcing functions is discussed relative to the dominant seasonal and interannual scales of variability for the wind-driven oceanic response. On seasonal time scales, critical differences in the wind stress products, of order 0.2–0.4 dynes cm^{-2}, were in wind regimes of surface convergence and significant gradients such as the ITCZ and SPCZ. These uncertainties in the wind fields were manifested in model sea level solutions as 6–12 cm discrepancies near the NECC Trough and east of New Guinea. On interannual time scales, the influence of greater sampling along the major ship tracks was evident. Away from the major shipping lanes rms differences in the wind stress anomalies (1979–1983) about the mean seasonal cycle (1979–1981) reached up to 0.5 dynes cm^{-2}. The combined effect of these differences in the wind products resulted in 8–20 cm rms differences in the model sea level simulations. The largest of these discrepancies tended to exist at the terminus of equatorial wave characteristics, e.g. in the east along the equator and in the west off the equator.

Butterfield, D.A., G.J. MASSOTH, R.E. McDuff, J.E. Lupton, and M.D. Lilley. Geochemistry of hydrothermal fluids from Axial Seamount Hydrothermal Emissions Study Vent Field, Juan de Fuca Ridge: Subseafloor boiling and subsequent fluid-rock interaction. *Journal of Geophysical Research, 95*(B8), 12,895–12,921 (1990).

Hydrothermal fluids collected from the ASHES vent field in 1986, 1987, and 1988 exhibit a very wide range of chemical composition over a small area (~60 m in diameter). Compositions range from a 300°C, gas-enriched (285 mmol/kg CO_2), low-chlorinity (~33% of seawater) fluid to a 328°C, relatively gas-depleted (50 mmol/kg CO_2), high-chlorinity (~116% of seawater) fluid. The entire range of measured compositions at ASHES is best explained by a single hydrothermal fluid undergoing phase separation while rising through the ocean crust, followed by partial segregation of the vapor and brine phases. Other mechanisms proposed to produce chlorinity variations in hydrothermal fluids (precipitation/dissolution of a chloride-bearing mineral or crustal hydration) cannot produce the covariation of chlorinity and gas content observed at ASHES. There is good agreement of the measured fluid compositions with compositions generated by a simple model of phase separation, in which gases are partitioned according to Henry's law and all salt remains in the liquid phase. Significant enrichments in silica, lithium and boron in the low-chlorinity fluids over levels predicted by the model are attributed to fluid-rock interaction in the upflow zone. Depletions in iron and calcium suggest that these elements have been removed by iron-sulfide and anhydrite precipitation at some time in the history of the low-chlorinity fluids. The distribution of low- and high-chlorinity venting is consistent with mechanisms of phase segregation based on differential buoyancy or relative permeability. The relatively

outside the sill in the Strait of Juan de Fuca estuary appear to be the result of storms on the Pacific Coast causing reversals of surface flow and variations in deep flow more than 135 km from the coast. Previous observations have shown deep salinity variations midway along the Strait, but these are the first to show this effect can penetrate the full length of the Strait causing near-bottom salinity variations of sufficient magnitude to influence flow into Puget Sound. This influence probably occurs from the onset of storms in autumn through subsidence in spring, although occasional large storms occur in summer. Although Puget Sound is more characteristic of a fjord, the simple model calculations here suggest similar processes may occur in lower-layer flow at the mouth of coastal plain estuaries.

CANNON, G.A., and D.J. PASHINSKI. Circulation near Axial Seamount. *Journal of Geophysical Research, 95*(B8), 12,823–12,828 (1990).

Year-long moored current measurements from 1987 to 1988 on the saddle (1860 m) between Axial Volcano and Brown Bear Seamount show an oscillating flow with a broadband frequency centered at about 4 days and a long-term average flow of about 4 cm/s southward. The measurements at sill depth also suggest a possible alternating exchange of water north and south of the Cobb-Eickelberg seamount chain with warmer water (0.05°C) coming from the north. However, measurements near the top of the volcano at about 1400 m show a weaker, but northward, mean flow, and the 4-day oscillation barely exists. Conductivity, temperature, and depth (CTD) observations on the east side of the volcano infer possible intensification of southward flow adjacent to the Juan de Fuca Ridge, similar to that found with combined CTD and current meter observations about 100 km to the south. Southward flow is hypothesized along the entire east side of the ridge. On the west side the Axial-Brown Bear saddle may be near a convergence zone between southward and northward currents which then flow westward. The highly energetic environment on the saddle suggests other gaps in the ridge, and seamount chains may be important in determining the fate of the hydrothermal effluents. The general oceanic flow at the top of the caldera, however, is more tenuous, and the depth of change between these two regimes cannot be determined.

COKELET, E.D., R.J. Stewart, and C.C. Ebbesmeyer. The annual mean transport in Puget Sound. NOAA TM ERL PMEL-92 (NTIS not yet available), 59 pp. (1990).

Puget Sound is modeled as a branched system of two-layered advective reaches separated by mixing zones. Fresh water and salt provide convenient tracers to calculate the annual mean layer transports. The technique utilizes historical records (1951–1956) of runoff and salinity which are analyzed with the aid of modern (principally 1970's) current meter records to provide the appropriate mass conserving landward- and seaward-flowing layer salinities for each reach. This is the first time that the long-term transports have been estimated simultaneously for the entire Strait of Juan de Fuca/Puget Sound system. With few exceptions the inferred transports agree well with estimates derived from scattered, shorter duration current observations. Uncertainties in the transports are estimated from uncertainties in the runoff, velocity profiles and salinities. The results provide the basis for

shallow depth of the seafloor (1540 m) and the observed chemistry of ASHES fluids are consistent with phase separation in the sub-critical or near-critical region.

CANNON, G.A. Puget Sound circulation: What have observations taught us, and what is still to be ascertained? Oceans '89 Proceedings, Seattle, WA, September 18–21, 1989, Vol. 1: Fisheries, Global Ocean Studies, Marine Policy and Education, Oceanographic Studies. Marine Technology Society, IEEE Publication Number 89CH2780-5, 77–80 (1989).

Understanding circulation and mixing within the Puget Sound estuarine system is important in assessing the fate of natural and man-induced contaminants. The water ultimately either transports contaminants out of the system or redistributes them within it. Research over the past twenty years has focused on directly measuring circulation in sufficient detail to determine the physical processes causing the dominant space and time variations of the flow. This paper summarizes some of our understanding of the estuarine circulation in the central part of the main basin of Puget Sound adjacent to Elliott Bay, some of our uncertainties, and future research needs. This part of Puget Sound has not received sufficient attention.

CANNON, G.A. Variations in horizontal density gradient forcing at the mouth of an estuary. In *Coastal and Estuarine Studies*, Vol. 38, R.T. Cheng (ed.). Springer-Verlag, New York, 375–388 (1990).

Puget Sound is a fjord-like estuary in which bottom-water intrusions are a dominant circulation feature that play a major role in the replacement of water below sill depth within the estuary. New observations on the inside and outside of the entrance sill show that while intrusions occur during neap tides as previously thought, the onset of the intrusions occurs before the minimum in the neap tides. Calculations using a model with a balance between the longitudinal pressure gradient and vertical mixing suggest the onset is influenced by fluctuations in the horizontal density gradient caused by salinity variations across the sill. They also show that the resultant bottom inflow can be further modified by strong surface winds. Deep salinity changes seaward of the sill in the Strait of Juan de Fuca estuary appear to be the result of storms on the Pacific coast causing reversals of surface flow and variations in deep flow more than 135 km from the coast. Although Puget Sound is a glacially carved estuary, flow over the entrance sill in Admiralty Inlet has characteristics which resemble coastal plain estuaries; thus, these studies may have more general applications to time variations in lower layer flow at the mouth of other estuaries.

CANNON, G.A., J.R. HOLBROOK, and D.J. PASHINSKI. Variations in the onset of bottom-water intrusions over the entrance sill of a fjord. *Estuaries, 13*(1), 31–42 (1990).

Puget Sound is a fjord-like estuary and bottom-water intrusions are major circulation features which play a dominant role in the replacement of water below sill depth. New observations on the inside and outside of the entrance sill show that, while intrusions occur during neap tides as previously thought, tne onset of the intrusions is a result of fluctuations in the horizontal density gradient caused by salinity variations across the sill. Salinity changes

outside the sill in the Strait of Juan de Fuca estuary appear to be the result of storms on the Pacific Coast causing reversals of surface flow and variations in deep flow more than 135 km from the coast. Previous observations have shown deep salinity variations midway along the Strait, but these are the first to show this effect can penetrate the full length of the Strait causing near-bottom salinity variations of sufficient magnitude to influence flow into Puget Sound. This influence probably occurs from the onset of storms in autumn through subsidence in spring, although occasional large storms occur in summer. Although Puget Sound is more characteristic of a fjord, the simple model calculations here suggest similar processes may occur in lower-layer flow at the mouth of coastal plain estuaries.

CANNON, G.A., and D.J. PASHINSKI. Circulation near Axial Seamount. *Journal of Geophysical Research, 95*(B8), 12,823–12,828 (1990).

Year-long moored current measurements from 1987 to 1988 on the saddle (1860 m) between Axial Volcano and Brown Bear Seamount show an oscillating flow with a broadband frequency centered at about 4 days and a long-term average flow of about 4 cm/s southward. The measurements at sill depth also suggest a possible alternating exchange of water north and south of the Cobb-Eickelberg seamount chain with warmer water (0.05°C) coming from the north. However, measurements near the top of the volcano at about 1400 m show a weaker, but northward, mean flow, and the 4-day oscillation barely exists. Conductivity, temperature, and depth (CTD) observations on the east side of the volcano infer possible intensification of southward flow adjacent to the Juan de Fuca Ridge, similar to that found with combined CTD and current meter observations about 100 km to the south. Southward flow is hypothesized along the entire east side of the ridge. On the west side the Axial-Brown Bear saddle may be near a convergence zone between southward and northward currents which then flow westward. The highly energetic environment on the saddle suggests other gaps in the ridge, and seamount chains may be important in determining the fate of the hydrothermal effluents. The general oceanic flow at the top of the caldera, however, is more tenuous, and the depth of change between these two regimes cannot be determined.

COKELET, E.D., R.J. Stewart, and C.C. Ebbesmeyer. The annual mean transport in Puget Sound. NOAA TM ERL PMEL-92 (NTIS not yet available), 59 pp. (1990).

Puget Sound is modeled as a branched system of two-layered advective reaches separated by mixing zones. Fresh water and salt provide convenient tracers to calculate the annual mean layer transports. The technique utilizes historical records (1951–1956) of runoff and salinity which are analyzed with the aid of modern (principally 1970's) current meter records to provide the appropriate mass conserving landward- and seaward-flowing layer salinities for each reach. This is the first time that the long-term transports have been estimated simultaneously for the entire Strait of Juan de Fuca/Puget Sound system. With few exceptions the inferred transports agree well with estimates derived from scattered, shorter duration current observations. Uncertainties in the transports are estimated from uncertainties in the runoff, velocity profiles and salinities. The results provide the basis for

future computations of refluxing and the steady state tracer concentrations and ages in the Sound.

Davison, J., and D.E. HARRISON. A day-to-day comparison study of Seasat scatterometer winds with winds observed from islands in the tropical Pacific. NOAA TM ERL PMEL-91 (NTIS PB90-158791), 71 pp. (1989).

The Seasat scatterometer observed near-surface vector winds over the world ocean from an 800-km orbit by measuring radar backscatter from the wind-roughened surface. The early end of the mission in 1978 forestalled some of the planned ground-truth validation experiments; questions remain about the instrument's performance, in particular away from mid-latitudes. To increase the geographical range of SASS and *in situ* comparison experiments, we have compared data from islands in the tropical Pacific and contemporaneous scatterometer winds. We used satellite winds derived from two different wind vector algorithms (the signal processing that reduces the radar backscatter to wind speed and direction). The SASS-2 algorithm due to Wentz provides clearly better agreement in wind speed than the earlier SASS-1 algorithm. SASS-1 speeds tend to be higher than the island measurements by about 1 m s^{-1} while daily mean SASS-2 minus island wind speed differences average –0.07 m s^{-1} over the islands. RMS differences between SASS-2 and the daily mean island data average 1.7 m s^{-1}; the SASS-1 RMS differences average 2.2 m s^{-1}. Because the Seasat wind algorithms yield solutions with more than one possible direction, a single direction can only be selected from the others using ancillary information. We compared direction results from the objective selection method developed at the Goddard Laboratory for Atmospheres, as well as results from the somewhat artificial method of selecting the SASS direction closest in agreement with the comparison island direction. When averaged over tens of days the Goddard directions agree closely with the island observations. However, Goddard daily average directions exhibit considerably higher variance than those measured at the islands. The closest direction technique gives daily mean SASS minus island RMS direction differences averaging 20 degrees over the nine islands; the Goddard RMS differences average 52 degrees. Day-to-day comparison figures of vector winds from GLA SASS-1 and the islands permit detailed examination of the SASS-derived wind fields in the tropical Pacific near the comparison islands.

Davison, J., and D.E. HARRISON. Comparison of Seasat scatterometer winds with tropical Pacific observations. *Journal of Geophysical Research, 95*(C3), 3403–3410 (1990).

The Seasat-A satellite scatterometer (SASS) observed near-surface vector winds over the world ocean from an 800-km orbit by measuring radar backscatter from the wind-roughened surface. The early end of the mission in 1978 forestalled some of the planned ground-truth validation experiments; questions remain about the instrument's performance, in particular away from mid-latitudes. To increase the geographical range of SASS and in situ comparison experiments, we have compared data from nine islands in the tropical Pacific and contemporaneous scatterometer winds. We used satellite winds derived from two different wind vector algorithms (the signal processing that reduces the radar backscatter to wind speed and direction). The SASS-2 algorithm due to Wentz provides clearly better agreement

in wind speed than the earlier SASS-1 algorithm. SASS-1 speeds tend to be higher than the island measurements by about 1 m s^{-1}, while daily mean SASS-2 minus island wind speed differences average –0.07 m s^{-1}. The rms differences between SASS-2 and the daily mean island data average 1.7 m s^{-1}; the SASS-1 rms differences average 2.2 m s^{-1}. Because the Seasat wind algorithms yield solutions with more than one possible direction, a single direction can only be selected from the others using ancillary information. We compared direction results from the objective selection method developed at the Goddard Laboratory for Atmospheres, as well as results from the somewhat artifical method of selecting the SASS direction closest in agreement with the comparison island direction. When averaged over tens of days the Goddard directions agree closely with the island observations. However, Goddard daily mean directions exhibit considerably higher variance than those measured at the islands. The closest direction technique gives daily mean SASS minus island rms direction differences averaging 20°; the Goddard rms differences average 52°.

EMBLEY, R.W., K.M. MURPHY, and C.G. FOX. High-resolution studies of the summit of Axial Volcano. *Journal of Geophysical Research, 95*(B8), 12,785–12,812 (1990).

Sea Beam bathymetry, Sea MARC I side scan (30 kHz), towed camera, and submersible data from Axial Volcano, Juan de Fuca Ridge (JdFR) have been integrated to produce detailed maps of the volcano's summit region in order to elucidate its volcanic and tectonic evolution. The proximity of Axial Volcano, the youngest edifice of the Cobb-Eickelberg Seamount Chain, to the JdFR superposes a hotspot-derived radial stress pattern onto the linear stress field of a mid-ocean ridge spreading center. The morphology of the summit of Axial Volcano reflects the differing eruptive styles produced from this superposition. Long rift zones begin at the edges of the caldera and extend as much as 75 km to the north and south. Axial Volcano has a distinct summit plateau similar to those found on many other submarine volcanos. The process by which summit plateaus are constructed is illustrated by the lava flows originating from the South Rift Zone, which have partially filled the southern half of the caldera and have smoothed the flanks. The summit plateau contains penetrative NE-SW fracturing that is approximately parallel to the JdFR. The unusual rectangular caldera is 3 × 8 km in size, and its trend is about 160°. Three possible mechanisms are discussed for the caldera's formation: (1) Canary Island-type "trapdoor" formation, (2) overlapping spreading center interaction, and (3) magma source migration. Although none of these models is fully compatible with the present data base, the overlapping spreading center model is preferred. Postcaldera volcanism probably began with the formation of the Central Caldera Eruptive Complex, which was characterized by relatively low-volume, high-viscosity flows. The most recent volcanism has apparently taken place along the northern and southern rift zones, which have erupted more fluid lavas resulting in areally extensive flows covering up to 60% of the caldera floor. Extensive low-temperature venting and areas of high-temperature venting near the northern and southern rift zones and caldera walls suggest a shallow magmatic source beneath the summit of Axial Volcano.

FEELY, R.A., T.L. GEISELMAN, E.T. BAKER, G.J. MASSOTH, and S.R. HAMMOND. Distribution and composition of hydrothermal plume particles from the ASHES vent field at Axial Volcano, Juan de Fuca Ridge. *Journal of Geophysical Research, 95*(B8), 12,855–12,873 (1990).

In 1986 and 1987, buoyant and neutrally buoyant hydrothermal plume particles from the ASHES vent field within Axial Volcano were sampled to study their variations in composition with height above the seafloor. Individual mineral phases were identified using standard X ray diffraction procedures. Elemental composition and particle morphologies were determined by X ray fluorescence spectrometry and scanning electron microscopy/X ray energy spectrometry techniques. The vent particles were primarily composed of sphalerite, anhydrite, pyrite, pyrrhotite, chalcopyrite, barite, hydrous iron oxides, and amorphous silica. Grain size analyses of buoyant plume particles showed rapid particle growth in the first few centimeters above the vent orifice, followed by differential sedimentation of the larger sulfide and sulfate minerals out of the buoyant plume. The neutrally buoyant plume consisted of a lower plume, which was highly enriched in Fe, S, Zn, and Cu, and an upper plume, which was highly enriched in Fe and Mn. The upper plume was enriched in Fe and Mn oxyhydroxide particles, and the lower plume was enriched in suspended sulfide particles in addition to the Fe and Mn oxyhydroxide particles. The chemical data for the water column particles indicate that chemical scavenging and differential sedimentation processes are major factors controlling the composition of the dispersing hydrothermal particles. Short-term sediment trap experiments indicate that the fallout from the ASHES vent field is not as large as some of the other vent fields on the Juan de Fuca Ridge.

FEELY, R.A., G.J. MASSOTH, E.T. BAKER, J.P. Cowen, M.F. LAMB, and K.A. Krogslund. The effect of hydrothermal processes on midwater phosphorus distributions in the northeast Pacific. *Earth and Planetary Science Letters, 96*, 305–318 (1990).

The distributions of dissolved, particulate and sedimentary phosphorus were measured in the region of the Juan de Fuca Ridge to determine the impacts of hydrothermal processes on the phosphorus cycle in the oceans. Significant negative dissolved phosphate anomalies, ranging from 0 to 60 nmol/l, were observed in the water column at depths between 1900 and 2300 db. The largest anomalies (< –50 nmol/l) were observed within the ridge axis. Corresponding positive particulate phosphorus anomalies and high concentrations of sedimentary phosphorus were also observed to have striking concentration gradients increasing towards the ridge axis. These observations provide strong evidence that phosphorus is being stripped from solution by scavenging reactions. Analysis of the particulate samples employing transmission electron microscopy techniques indicates that the scavenging occurs on newly-formed iron oxyhydroxides of hydrothermal origin. Mass balance calculations suggest that up to 12% of the total annual phosphorus sink in the oceans is a result of scavenging by hydrothermal emissions.

FOX, C.G. Acoustic techniques for imaging the seafloor. In *Gorda Ridge: A Seafloor Spreading Center in the United States Exclusive Economic Zone*, G.R. McMurray (ed.). Springer-Verlag, New York, 169–178 (1990).

The recent development of sophisticated sonar systems for seafloor imaging allows analyses of terrain beyond simple bathymetric mapping. The SEABEAM multibeam sonar system produces full-coverage 12-kHz soundings, and much of the Gorda Ridge has been surveyed by the National Oceanic and Atmospheric Administration and the U.S. Navy. Complete-coverage digital bathymetry provides the basic data for statistical modeling of seafloor roughness through spectral and fractal mathematical techniques. In addition to soundings, the SEABEAM system can provide fundamental information about bottom properties through evaluation of the backscattered acoustical signal. Side-scan sonar systems allow more detailed observations of the variability of acoustic properties. Available side-scan sonar data range from the broad (60-km swath) complete coverage of the GLORIA system collected by the U.S. Geological Survey to 10-km swath SeaMARC II and 5- to 0.5-km-wide SeaMARC I imaging, which produces pixel spot sizes of as little as 25 cm. The full-coverage, digital nature of these data allows the application of terrain classification techniques developed for satellite imagery. The validity of remote-imaging techniques can only be evaluated when compared to observational ground truth. A recently developed technique for geological mapping from bottom photography facilitates such comparisons.

FOX, C.G. Consequences of phase separation on the distribution of hydrothermal fluids at ASHES vent field, Axial Volcano, Juan de Fuca Ridge. *Journal of Geophysical Research, 95*(B8), 12,923–12,926 (1990).

Recent studies of hydrothermal fluid chemistry at the Axial Seamount Hydrothermal Emissions Study (ASHES) vent field of Axial Volcano indicate separation of liquid and vapor phases during the migration of fluids to the seafloor. The brine phase liquid emanates from discrete sulfide chimneys, while fluid which has been through vapor phase separation flows diffusely from fissures in the surrounding basalt. One possible mechanism to explain this spatial segregation of the fluid phases is based on the relative permeability terms in the equations of two-phase flow. A qualitative model for the distribution of fluids observed at ASHES is postulated in which brine phase fluids are confined within flow conduits by a surrounding relative permeability barrier, while vapor phase fluids flow diffusely into the surrounding host rock.

FOX, C.G. Evidence of active ground deformation on the mid-ocean ridge: Axial Seamount, Juan de Fuca Ridge, April–June 1988. *Journal of Geophysical Research, 95*(B8), 12,813–12,822 (1990).

Since September 1987 a precision bottom pressure recorder (BPR) has been deployed within the summit caldera of Axial Seamount on the central Juan de Fuca Ridge. The instrument is capable of measuring pressure to 1 mbar resolution and recording these measurements at 64 samples per hour for up to 15 months. After removal of oscillatory signals due to tidal and oceanographic effects and linear trends caused by sensor drift, any significant change in the pressure record should indicate a change of depth associated with vertical ground

movement. In subaerial volcanic systems, such ground movements commonly indicate active inflation or deflation of underlying magma bodies and are frequently coincident with rift eruptions. Axial Seamount was selected for this pilot study for three primary reasons: (1) its tectonic setting, (2) the presence of a well-formed summit caldera, and (3) observational evidence of geologically recent volcanic activity. Results from the first 9 months of the BPR deployment revealed a significant change in pressure, which is interpreted to represent a 15-cm subsidence of the caldera floor during two 2- to 3-week periods in April-June 1988. Also during these periods, an anomalous decline in temperature at the site was recorded that is correlated with an apparent increase in current velocity at the Axial Seamount Hydrothermal Emissions Study (ASHES) vent field, suggesting vigorous advection of cold water into the caldera. Concurrent oceanographic data from Geosat and from current meter arrays do not indicate any large-scale oceanographic phenomena capable of generating these simultaneous events. One mechanism to explain simultaneous ground subsidence and temperature decline at the caldera center and increased bottom current at the caldera margin is the generation of a buoyant parcel of heated water in response to the intrusion or the eruption of magma associated with volcanic deflation. Such a parcel must have been sufficiently buoyant and proximal to induce horizontal entrainment currents capable of producing the bottom water conditions that were observed at both sites. Similar volcanic events also may have generated large midwater plumes that have been described previously along the southern Juan de Fuca Ridge.

FOX, C.G., F.J. JONES, and T.-K. Lau. Constrained iterative deconvolution applied to SeaMARC I sidescan sonar imagery. *IEEE Journal of Oceanic Engineering, 15*(1), 24–31 (1990).

Images collected by any sidescan sonar system represent the convolution of the acoustic beam pattern of the instrument with the true echo amplitude distribution over the seafloor. At typical tow speeds, the 1.7° beam width of SeaMARC I results in multiple insonification of individual targets, particularly at the outside of the swath. A nonlinearly constrained iterative deconvolution technique developed for radar applications can be applied to SeaMARC I imagery to reduce the effect of the beam pattern and equalize the spectral content of the image across the swath. Since the deconvolution is implemented in the along-track direction, the registration of individual scan lines must be precisely corrected before the operator is applied. The deconvolution operator must be modeled to account for beam shape, vehicle speed, swath width, slant range, and ping rate. The method is numerically stable and increases the effective resolution of the image, but results in some loss of dynamic range. The technique is applied to target recognition and imagery from volcanic terrains of the central Juan de Fuca Ridge.

Giese, B.S., and D.E. HARRISON. Aspects of the Kelvin wave response to episodic wind forcing. *Journal of Geophysical Research, 95*(C5), 7289–7312 (1990).

Episodes of westerly wind are an important aspect of surface stress variability in the western Pacific. During El Niño-Southern Oscillation periods, the presence of such wind episodes comprises much of the low-frequency relaxation of the trades over the central and western Pacific. In this paper we describe the oceanic Kelvin pulse response to a single idealized

episode of westerly wind stress, using results from linear theory as well as from a 27-level general circulation model. Linear theory predicts that an episode of westerly wind will excite a train of equatorial trapped Kelvin pulses. The amplitude and longitudinal structure of the forced ocean Kelvin pulses varies as a function of baroclinic mode and the wind patch properties. Because of changing vertical thermal structure across the Pacific, the vertical structure of Kelvin pulses is altered as they propagate away from the forcing region. When stratification typical of the western and eastern Pacific is used, the conservation of energy flux predicts a reduction of surface currents associated with the first baroclinic mode and an enhancement of surface currents associated with the second baroclinic mode. The idealized wind anomaly is also used to drive an ocean general circulation model. When the wind anomaly is weak the model Kelvin response agrees with predictions of linear theory. For more realistic strong forcing there are three important deviations from linear theory: the amplitude of low baroclinic modes increases; the amplitude of higher baroclinic modes decreases; and the phase speed increases. In the presence of realistic oceanic background conditions, response in the equatorial waveguide is complicated by the equatorial undercurrent, a sloping thermocline and instability waves. Model sea surface temperature warming at the coast of South America is dominated by the second baroclinic mode, consistent with the results derived from linear theory.

GONZALEZ, F.I., and E.N. BERNARD. Deep ocean tsunami and seismic wave observations: Three recent Gulf of Alaska events. Proceedings of Workshop XLVI, The 7th U.S.-Japan Seminar on Earthquake Prediction, Menlo Park, CA, 12–15 September 1988. USGS Open-File Report 90-98, 131–134 (1990).

No abstract.

HAMMOND, S.R. Relationships between lava types, seafloor morphology, and the occurrence of hydrothermal venting in the ASHES vent field of Axial Volcano. *Journal of Geophysical Research, 95*(B8), 12,875–12,893 (1990).

Deep-towed and submersible photographic surveys within the caldera of Axial Volcano have been integrated with high-resolution bathymetry to produce a geological map of the most active vent field (Axial Seamount Hydrothermal Expeditions (ASHES)) in the caldera. The ASHES vent field encompasses an approximately 200 m × 1200 m area of active venting which is located adjacent to the southwest caldera wall. Locations for over 2000 photographs in and near the vent field were determined using a seafloor transponder network. Then each photograph was described utilizing a classification system which provides detailed information concerning lava type, hydrothermal activity, sediment cover, geological structure, and biology. Resulting data were entered into a digital data base, and computer-generated maps were created that portray spatial relationships between selected geological variables. In general, the entire ASHES field is characterized by pervasive low-temperature venting. The most vigorous venting is concentrated in an approximately 80 m × 80 m area where there are several high-temperature vents including some which are producing high-temperature vapor-phase fluids derived from a boiling hydrothermal system. Lava types within the ASHES vent field are grouped into three distinct morphologies: (1) smooth (flat-surfaced,

ropy, and whorled) sheet flows, (2) lobate flows, and (3) jumbled-sheet flows. The most intense hydrothermal venting is concentrated in the smooth sheet flows and the lobate flows. The location of the ASHES field is mainly attributable to faulting which defines the southwest caldera wall, but the concentration of intense venting appears to be related also to the spatial distribution of lava types in the vent field and their contrasting permeabilities. Other structural trends of faults and fissures within the field also influence the location of individual vents.

HARRISON, D.E. Post World War II trends in tropical Pacific surface trades. *Journal of Climate,* 2(12), 1561–1563 (1989).

Multidecadal time series of surface winds from central tropical Pacific islands are used to compute trends in the trade winds between the end of WWII and 1985. Over this period, averaged over the whole region, there is no statistically significant trend in speed of zonal or meridional wind (or pseudostress). However, there is some tendency, within a few degrees of the equator, toward weakening of the easterlies and increased meridional flow toward the equator. Anomalous conditions subsequent to the 1972–73 ENSO event make a considerable contribution to the long-term trends. The period 1974–80 has been noted previously to have been anomalous, and trends over that period are sharply greater than those over the longer records.

HARRISON, D.E., B.S. Giese, and E.S. Sarachik. Mechanisms of SST change in the equatorial waveguide during the 1982–83 ENSO. *Journal of Climate, 3*(2), 173–188 (1990).

Four different datasets of monthly mean near-equatorial Pacific sea surface temperature for 1982–83 are compared, and the space-time regions for which there was consensus that cooling or warming took place, are determined. There was consensus that warming took place east of the date line, averaged over the period July-December 1982, and that the warming progressed eastward from the central Pacific. There was also consensus that weak cooling took place in April 1983, and that substantial cooling occurred in June-July 1983, generally over the central and eastern Pacific. However, the analyses tend to agree on the sign of SST change only in periods of cooling or warming in excess of 1°C/month; quantitative agreement at the level of 0.5°C/month or better is almost never found. SST changes in five ocean-circulation model hindcasts of the 1982–83 period (differing only in that each used a different analyzed monthly mean surface wind stress field to drive the ocean), are compared with the observations and with each other. There is agreement that net warming occurred in the July–December 1982 period and cooling in mid-1983. The heat budgets of these experiments indicate that the major model central Pacific warmings occurred primarily from anomalous eastward surface advection of warm water. Further, east zonal advection remains significant, but a diminished cooling tendency from meridional advection can also be important; different hindcasts differ on the relative importance of these terms. Surface heat flux changes do not contribute to the warmings. The reduced cooling tendency from meridional advection is consistent with diminished surface Ekman divergence, suggesting that southward transport of warm north equatorial counter current water was not a major factor in the model warmings. The hindcasts do not agree on the relative importance of local or remote forcing

of the eastward surface currents; while there is clear evidence of remote forcing in some hindcasts in particular regions, local forcing is also often significant. The main 1983 midocean cooling began because of increased vertical advection of cool water; but once cooling began horizontal advection often contributed. Further east, where the easterlies generally return later than they do in midocean, upwelling and horizontal advection all can be important. Again no model consensus exists concerning the details of SST evolution. Because the observations do not agree on the sign of SST change during much of the 1982–83 period, improved SST data is needed in order to document the behavior of the ocean through future ENSO periods. Better forcing data will be needed to carry out improved ocean-model validation studies, and to explore the mechanisms likely responsible for SST change through entire ENSO cycles.

HARRISON, D.E., and D.S. Luther. Surface winds from tropical Pacific islands—climatological statistics. *Journal of Climate, 3*(2), 251–271 (1990).

Multidecadal time series of surface wind observations from tropical Pacific islands have been examined in order to investigate the space and time scales of variability. Climatological monthly means and variances are compared with comparable means and variances derived from ship observations; usually the means agree to within ~1 m s^{-1} in speed and ~10 degrees in direction. Annual and semiannual cycles differ in detail. Island zonal wind variances are often significantly larger, by up to 10 m^2 s^{-2} near the equator between September and December; because of the spatial coherence of the island results, these discrepancies are believed to result from the poor high-frequency sampling typical of ship data. A substantial near-equatorial zonal wind variance maximum is shown to be related to ENSO period variability; excluding ENSO time periods leaves a relatively spatially uniform variance of ~5 m^2 s^{-2} over a broad region. The frequency distribution of variance, derived from daily-averaged data, exhibits considerable geographical variation. Within a few degrees of the equator the most energetic zonal wind variability is found in a broad band extending from about 3- to 60-day periods, with maximum at about 10 days; there is also significant interannual power in records located west of 170°W. There is occasionally a local variance maximum in the range of 30- to 60-day periods. Within this near-equatorial region, the meridional wind variance is roughly half the zonal wind variance and is found primarily between about 3-day and 6-day periods and at the annual period. Poleward of about 5 degrees of latitude, the interannual variability in zonal wind diminishes sharply, and the zonal and meridional wind variances become increasingly comparable. The zonal wind energy level in the 3- to 60-day band decreases as one moves farther from the equator, until the more energetic winds typical of subtropical latitudes arise. Coherence calculations typically show zonal wind coherence significant at the 95% level at all energetic periods when islands are within 200–300 km of each other meridionally, and within 1000–1500 km zonally. The meridional wind tends to be less coherent. A minimal sampling array for tropical surface wind variability in this region should have meridional sampling about every 2° and zonal sampling about every 15° for the zonal wind, and perhaps half these distances for the meridional wind.

HAYES, S.P. The Tropical Atmosphere Ocean Array—TOGA-TAO. Proceedings of the International Symposium on Japanese Pacific Climate Study (JAPACS), Center for Institutes, Tsukuba City, Japan, October 19–20, 1989, 67-1 to 67-3 (1989).

No abstract.

HAYES, S.P., M.J. MCPHADEN, and J.M. Wallace. The influence of sea-surface temperature on surface wind in the eastern equatorial Pacific: Weekly to monthly variability. *Journal of Climate,* 2(12), 1500–1506 (1989).

Temporal correlations between near-equatorial surface wind and sea-surface temperatures (SST) at 110°W in the eastern Pacific Ocean are investigated using data from an array of moored sensors between 5°N and 5°S. The signature of tropical instability waves with periods of 20–30 days is apparent in time series of SST and both the meridional and zonal wind components. Results indicate the existence of a band of pronounced horizontal divergence in the surface wind field associated with the large meridional SST gradient (equatorial front) normally located just north of the equator. Perturbations of the equatorial front by the instability waves induce fluctuations in the overlying winds. Evidence of the air-sea coupling is stronger in time series of the meridional gradients of wind and SST than between time series of the variables themselves. The meridional differencing serves as a high-pass filter in the space domain, which removes planetary-scale wind fluctuations that are unrelated to the local SST perturbations. The wind fluctuations observed in association with tropical instability waves are on the order of 1–2 m s^{-1}. These results indicate that SST variability on weekly to monthly time scales forces perturbations in the surface wind field. It is suggested that the principal coupling mechanism in this region is the modification of the atmospheric boundary layer stratification. Over the equatorial cold SST tongue the vertical wind shear within the lowest 100 m of the atmosphere is strong and the surface winds are conspicuously weak. As the air flows northward across the equatorial front the boundary layer becomes destabilized, momentum is mixed downward, and the surface winds increase.

HAYES, S.P., M.J. MCPHADEN, J.M. Wallace, and J. Picaut. The influence of sea-surface temperature on surface wind in the equatorial Pacific Ocean. Proceedings of the Western Pacific International Meeting and Workshop on TOGA COARE, Nouméa, New Caledonia, May 24–30, 1989. ORSTOM, 543–547 (1989).

No abstract.

Hildebrand, J.A., J.M. Stevenson, P.T.C. Hammer, M.A. Zumberge, R.L. Parker, C.G. FOX, and P.J. MEIS. A seafloor and sea surface gravity survey of Axial volcano. *Journal of Geophysical Research, 95*(B8), 12,751–12,763 (1990).

Seafloor and sea surface gravity measurements are used to model the internal density structure of Axial Volcano. Seafloor measurements made at 53 sites within and adjacent to the Axial Volcano summit caldera provide constraints on the fine-scale density structure.

Shipboard gravity measurements made along 540 km of track line above Axial Volcano and adjacent portions of the Juan de Fuca ridge provide constraints on the density over a broader region and on the isostatic compensation. The seafloor gravity anomalies give an average density of 2.7 g cm^{-3} for the uppermost portion of Axial Volcano. The sea surface gravity anomalies yield a local compensation parameter of 23%, significantly less than expected for a volcanic edifice built on zero age lithosphere. Three-dimensional ideal body models of the seafloor gravity measurements suggest that low-density material, with a density contrast of at least 0.15 g cm^{-3}, may be located underneath the summit caldera. The data are consistent with low-density material at shallow depths near the southern portion of the caldera, dipping downward to the north. The correlation of shallow low-density material and surface expressions of recent volcanic activity (fresh lavas and high-temperature hydrothermal venting) suggests a zone of highly porous crust. Seminorm minimization modeling of the surface gravity measurements also suggest a low-density region under the central portion of Axial Volcano. The presence of low-density material beneath Axial caldera suggests a partially molten magma chamber at depth.

Huebert, B.J., T.S. BATES, A. Bandy, S. Larsen, and R.A. Duce. Planning for chemical air-sea exchange research. *Eos, Transactions of the American Geophysical Union, 71*(35), 1051–1057 (1990).

No abstract.

Incze, L.S., P.B. Ortner, and J.D. SCHUMACHER. Microzooplankton, vertical mixing and advection in a larval fish patch. *Journal of Plankton Research, 12*(2), 365–379 (1990).

A large (~30 × 75 km) patch of larval walleye pollock, *Theragra chalcogramma*, was located south of the Alaska Peninsula during May 1986. A drifter deployed in this patch followed an anticyclonic path consistent with dynamic topography. Changes in community composition and vertical distribution of microzooplankton >40 μm were sampled for 4 days alongside this drifter to examine feeding conditions for larvae. Biological and physical changes during the first 2 calm days revealed substantial small-scale variability within the larger circulation pattern. Changes during the last 2 days were dominated by vertical mixing due to strong winds. Despite mixing, prey concentrations remained adequate for feeding by larval pollock as determined by laboratory studies. A satellite-tracked drifter replaced the first drifter and was still located within the patch 6 days later. Overall distributions of larvae and movements of the drifters show a net translation of 7.8 km day^{-1} south-westward, but details of the study reveal complex interactions between coastal waters and a coastal current. During the 10-day period there was an increase in standard length of the larval fish population of 0.13 mm day^{-1} and a decline in abundance of ~7.6% day^{-1}. Both calculated rates must be underestimates due to continuing recruitment of small larvae from hatching eggs.

Johnson, H.P., and R.W. EMBLEY. Axial Seamount: An active ridge axis volcano on the central Juan de Fuca Ridge. *Journal of Geophysical Research, 95*(B8), 12,689–12,696 (1990).

No abstract.

Johnson, J.E., R.H. GAMMON, J. LARSEN, T.S. BATES, S.J. Oltmans, and J.C. Farmer. Ozone in the marine boundary layer over the Pacific and Indian Oceans: Latitudinal gradients and diurnal cycles. *Journal of Geophysical Research, 95*(D8), 11,847–11,856 (1990).

Ozone concentrations in the atmospheric boundary layer of the Pacific and Indian Oceans were measured on four separate oceanographic research cruises (July 1986, May to August 1987, April to May 1988). These measurements show a distinct zone of near zero (≤3 ppb) ozone concentration in the central equatorial Pacific in April-May, with ozone increasing in this region over the next 4 months. The seasonal observed change in the latitudinal gradient of ozone is consistent with previous ozone measurements at Hilo and Samoa by *Oltmans and Komhyr* [1986] and predictions from an atmospheric general circulation model study [*Levy et al.*, 1985]. A significant diurnal cycle of ozone was found in almost all locations with a maximum near sunrise, a minimum in the late afternoon, and a peak-to-peak amplitude of 1 to 2 ppb (10–20%), similar to that predicted by a photochemical model in the low NO_x limit [*Thompson and Lenschow*, 1984].

Kessler, W.S. Observations of long Rossby waves in the northern tropical Pacific. *Journal of Geophysical Research, 95*(C4), 5183–5217 (1990).

Long baroclinic Rossby waves are potentially important in the adjustment of the tropical Pacific pycnocline to both annual and interannual wind stress curl fluctuations. Evidence for such waves is found in variations of the depth of the 20°C isotherm in the northern tropical Pacific during 1970–1987. A total of 199,067 bathythermograph profiles have been compiled from the archives of several countries; the data coverage is dense enough that westward propagating events may be observed with a minimum of zonal interpolation. After extensive quality control, 20°C depths were gridded with a resolution of 2° latitude, 5° longitude, and bimonths; statistical parameters of the data were estimated. A simple model of low-frequency quasi-geostrophic pycnocline variability allows the physical processes of Ekman pumping, the radiation of long (nondispersive) Rossby waves due to such pumping in midbasin, and the radiation of long Rossby waves from the observed eastern boundary pycnoline depth fluctuations. Although the wind stress curl has very little zonal variability at the annual period in the northern tropical Pacific, an annual fluctuation of 20°C depth propagates westward as a long Rossby wave near 5°N and 14°–18°N in agreement with the model hindcast. Near the thermocline ridge at 10°N, however, the annual cycle across the basin is dominated by local Ekman pumping. The wave-dominated variability at 5°N weakens the annual cycle of geostrophic transport of the North Equatorial Countercurrent in the western Pacific. El Niño events are associated with westerly wind anomalies concentrated in the central equatorial Pacific; upwelling wind stress curl is generated in the extraequatorial tropics by these westerlies. Long upwelling Rossby waves forced by this curl pattern were observed to raise the western Pacific thermocline well outside the equatorial waveguide in

the later stages of El Niños, consistent with the simple long-wave model. The observations suggest that although simple reflection of the long Rossby waves from the western boundary is not the major process affecting subsequent development on the equator, it is likely that the extraequatorial waves play some role in setting the timescale of ENSO events.

Kiene, R.P., and T.S. BATES. Biological removal of dimethyl sulphide from sea water. *Nature, 345*(6277), 702–705 (1990).

Dimethyl sulphide (DMS) is an important sulphur-containing trace gas in the atmosphere. It is present in oceanic surface waters at concentrations sufficient to sustain a considerable net flux of DMS from the oceans to the atmosphere, estimated to comprise nearly half of the global biogenic input of sulphur to the atmosphere. DMS emitted from the oceans may be a precursor of tropospheric aerosols and of cloud condensation nuclei in the remote marine atmosphere, thereby affecting the Earth's radiative balance and thus its climate. Relatively little is known, however, about the biogeochemical and physical processes that control the concentration of DMS in sea water. Here we present data from incubation experiments, carried out at sea, which show that DMS is removed by microbial activity. In the eastern, tropical Pacific Ocean, DMS turnover is dominated by biological processes, with turnover times for biological DMS removal generally more than ten (3–430) times faster than turnover by ventilation to the atmosphere. Thus biological consumption of DMS seems to be a more important factor than atmospheric exchange in controlling DMS concentrations in the ocean, and hence its flux to the atmosphere. These results have significant implications for climate feedback models involving DMS emissions, and highlight the importance of the microbial food web in oceanic DMS cycling.

Landsteiner, M.C., M.J. MCPHADEN, and J. Picaut. On the sensitivity of Sverdrup transport estimates to the specification of wind stress forcing in the tropical Pacific. *Journal of Geophysical Research, 95*(C2), 1681–1691 (1990).

We use Sverdrup dynamics to estimate geostrophic transports between 20°N and 20°S in the tropical Pacific Ocean averaged over the period 1979–1981. Three wind stress products are used to force the model. Results are compared to geostrophic transports computed along expendable bathythermograph transects in the western, central, and eastern Pacific for the same period. Depending on the choice of wind stress, modeled transports may differ from the observations by a factor of 2 and, in some cases, flow is opposite to that observed. Possible limitations of the Sverdrup theory are discussed; however, we conclude that detailed and accurate simulation of the general circulation in the tropical Pacific is limited more by the uncertainties in presently available estimates of the surface wind stresses than by deviations from Sverdrup balance.

LARSEN, J.C. Transfer functions: Smooth robust estimates by least-squares and remote reference methods. *Geophysical Journal International, 99*, 645–663 (1989).

A method is described for finding the magnetotelluric transfer function that has the least amount of curvature consistent with most of the data and with a 1-D conductivity interpretation over the widest possible frequency range. This could be called an "Occam" transfer function. It is represented by the transfer function for the best fitting 1-D conductivity model times a distortion function. The latter permits smooth departures of the transfer function from the 1-D case if the data are inconsistent with a 1-D interpretation. The transfer function, for single-station or remote reference magnetotelluric data, is found by a method of successive iterations that is found to converge within six to eight iterations. The estimate of the transfer functions is made robust by using frequency and time weights that remove the effects of outliers in the time and frequency domain. If the weighted residuals for remote reference data satisfy certain necessary conditions for uncorrelated noise then the contribution to the noise by the electric and magnetic data can be estimated and used to evaluate the least-squares and remote reference estimates. Examples illustrate the application of this method to artificial and real data. The latter consist of hourly cable voltage data from the Florida Straits, 1/256-s remote reference magnetotelluric survey data from the Phillippines and daily magnetic data from Tucson and Honolulu.

LARSEN, J.C. Transport measurements from in service undersea telephone cables. Proceedings, Workshop on Scientific Uses of Undersea Cables, Honolulu, HI, Jan. 30–Feb. 1, 1990. Incorporated Research Institutions for Seismology (IRIS)/Joint Oceanographic Institutions (JOI), 117–130 (1990).

Eight years of continuous recordings of the voltages across the Florida Straits using an abandoned cable making ocean contact near Jupiter, Florida and Settlement Point, Grand Bahama Island, have shown that this is an inexpensive method for accurately monitoring the transport fluctuations of the Florida Current (Larsen & Sanford 1985, Larsen 1990). The conversion of the voltages to transports (24.30 ± 0.53 Sv/V) (1 Sverdrup = 1 Sv = 10^6 m^3/s) was determined by a comparison with 130 days of transport values derived from velocity profiling data. The rms misfit is 0.7 Sv which is about the accuracy of the profiling derived transports. Undersea telephone cables, including the new fiber optic cables, can also, in principle, be used to determine the voltage difference between the cable-ocean contacts by recording the power voltage and current. The success of the abandoned cable in monitoring the transport, the existence of undersea telephone cables and the expense of deploying new cables justifies a serious effort to investigate whether in service undersea telephone cables can be used for monitoring ocean currents.

Latif, M., J. Biercamp, H. von Storch, M.J. MCPHADEN, and E. Kirk. Simulation of ENSO related surface wind anomalies with an atmospheric GCM forced by observed SST. *Journal of Climate*, 3(5), 509–521 (1990).

The ECMWF-T21 atmospheric GCM is forced by observed near-global SST from January 1970 to December 1985. Its response in low level winds and surface wind stress over the Pacific

Ocean is compared with various observations. The time dependent SST clearly induces a Southern Oscillation (SO) in the model run which is apparent in the time series of all variables considered. The phase of the GCM SO is as observed, but its low frequency variance is too weak and is mainly confined to the western Pacific. Because of the GCM's use as the atmospheric component in a coupled ocean-atmosphere model, the response of an equatorial oceanic primitive equation model to both the modeled and observed wind stress is examined. The ocean model responds to the full observed wind stress forcing in a manner almost identical to that when it is forced by the first two low frequency EOFs of the observations only. These first two EOFs describe a regular eastward propagation of the SO signal from the western Pacific to the central Pacific within about a year. The ocean model's response to the modeled wind stress is too weak and similar to the response when the observed forcing is truncated to the first EOF only. In other words, the observed SO appears as a sequence of propagating patterns but the simulated SO as a standing oscillation. The nature of the deviation of the simulated wind stress from observations is analyzed by means of Model Output Statistics (MOS). It is shown that a MOS-corrected simulated wind stress, if used to force an ocean GCM, leads to a significant enhancement of low frequency SST variance, which is most pronounced in the western Pacific.

MANGUM, L.J., S.P. HAYES, J.M. Toole, Z. Wang, S. Pu, and D. Hu. Thermohaline structure and zonal pressure gradient in the western equatorial Pacific. *Journal of Geophysical Research, 95*(C5), 7279–7288 (1990).

Two recent sections of temperature and salinity along the equator in the western Pacific were examined in the context of the historical hydrographic data. Both sections occurred during the December-February period when climatological mean winds are northwesterly. The historical data indicate that the zonal sea surface slope responds to the seasonal change in wind stress. During the southeasterly monsoon the historical mean surface relative to 500 dbar dynamic height slopes upwards from east to west; during the northwesterly monsoon this slope reverses. Vertical profiles of the mean zonal pressure gradient relative to 500 dbar suggest that the wind influence may extend quite deep in the water column. The two quasi-synoptic sections both indicated that the sea level sloped downward towards the west between 155°E and 140°E. The sign of this slope agrees with the historical seasonal mean; however, the zonally averaged sea level in this westernmost region changed by nearly 0.1 dyn m between sections. Upper ocean water properties and stratification confirmed the importance of salinity in determining mixed layer depth. Comparisons of repeat stations collected during a 16-day period indicated relatively rapid changes in near surface properties and the importance of lateral advection.

Martin, D.C., D. BORG-BREEN, J.C. Martin, and A.P. Streissguth. Microcomputer measurement and analysis of newborn sucking. *Behavior Research Methods, Instruments, & Computers,* 22(4), 393–401 (1990).

An on-line Basic computer program with on-line monitor prompts and read-out collects, stores, and digitizes pressure and latency of sucking responses for later analyses. The program and analog equipment are described, and approximate costs are noted.

MCPHADEN, M.J. Comment on "Rossby-gravity waves in the central equatorial Pacific Ocean during the NORPAX Hawaii-to-Tahiti Shuttle Experiment" by S.M. Chiswell and R. Lukas. *Journal of Geophysical Research, 95*(C1), 805–806 (1990).

No abstract.

MCPHADEN, M.J. Moored equatorial current measurements in the Pacific Ocean. Proceedings of the International Symposium on Japanese Pacific Climate Study (JAPACS), Center for Institutes, Tsukuba City, Japan, 19–20 October 1989, 57-1 to 57-5 (1989).

No abstract.

MCPHADEN, M.J. On the relationship between winds and upper ocean temperature variability in the western equatorial Pacific. Proceedings of the Western Pacific International Meeting and Workshop on TOGA COARE, Nouméa, New Caledonia, May 24–30, 1989. ORSTOM, 283–290 (1989).

In this study we examine the relationship between winds and upper ocean temperature variability using data from an equatorial mooring at 0°, 165°E. The analysis focuses primarily on daily to monthly time scale variations during 1986 and 1987 at the height of the 1986–87 El Niño/Southern Oscillation event. The period is one of high mean sea surface temperatures ($\geq$29°C) and frequent outbreaks of westerly winds. We infer that in general wind-driven vertical advection and entrainment from the thermocline are not likely to be important processes affecting surface temperatures in the western equatorial Pacific. Conversely, we conclude that variations in evaporative cooling may account for a significant percentage of the observed surface layer temperature variance during the study period.

MCPHADEN, M.J., H.P. FREITAG, and A.J. SHEPHERD. Moored salinity time series measurements at 0°, 140°W. *Journal of Atmospheric and Oceanic Technology, 7*(4), 568–575 (1990).

This study describes moored salinity time series measurements in a biologically productive equatorial upwelling regime in the Pacific Ocean (0°, 140°W). Data were collected at 26 m and at 100 m for 13 months during 1987–1988 using four SEACAT conductivity and temperature recorders equipped with optional antifouling attachments. Laboratory pre- and post-deployment calibrations indicate that the instrumental drift in SEACAT salinity measurements was typically <0.015 psu with a maximum of 0.055 psu for sequential 6–7 month long mooring deployments. Root mean square (rms) differences with CTD casts taken within a few nautical miles of the moorings were ~0.05 psu. These values are an order of magnitude smaller than the observed range of salinity variations. Little biogenic material was found on the SEACAT sensors on recovery. Thus, we infer that the antifouling attachments used were effective and that similar favorable results using SEACATs can be expected at other times and places in equatorial upwelling regimes.

MCPHADEN, M.J., and S.P. HAYES. Variability in the eastern equatorial Pacific Ocean during 1986–1988. *Journal of Geophysical Research, 95*(C8), 13,195–13,208 (1990).

We examine variability in the eastern equatorial Pacific during 1986–1988 using conductivity-temperature-depth data, velocity and temperature data from equatorial moorings between 110°W and 140°W, and wind data from a basin scale zonal array of islands and moorings between 110°W and 165°E. The period studied coincides with the El Niño/Southern Oscillation (ENSO) event of 1986–1987 and a subsequent cold event in 1988. Weak warm sea surface temperature anomalies first appeared in the eastern equatorial Pacific in mid-1986 and increased to >1°C in September-November 1986 in association with a 30 cm s^{-1} weakening of the South Equatorial Current and a 20- to 40-m depression of the thermocline. These warm anomalies lasted until early 1988, after which a large-scale shoaling of the thermocline led to sea surface temperatures more than 3°C colder than climatology. Year-to-year fluctuations in the eastern Pacific were related primarily to zonal wind variations in the central and western Pacific. Westerly wind stress anomalies of 0.02–0.05 N m^{-2} were observed between 140°W and 165°E from the latter half of 1986 until the end of 1987; these were replaced by easterly wind anomalies of similar magnitude between 157°W and 165°E in 1988. Energetic intraseasonal fluctuations with periods of 2–3 months were also prominent in zonal current, temperature, and dynamic height time series. These fluctuations propagate eastward at approximately first baroclinic mode Kelvin wave phase speeds and are forced west of the date line by episodes of westerly winds. Extrema in several oceanic variables occurred in association with these waves, though their precise dynamical link to the ENSO cycle is unclear from our data. Sea surface temperature and thermocline depth anomalies at 0°, 110°W were less pronounced during the 1986–87 ENSO than during the 1982–83 ENSO; the Equatorial Undercurrent, though weaker than normal in early 1987, did not disappear as it did in early 1983.

MCPHADEN, M.J., S.P. HAYES, L.J. MANGUM, and J.M. Toole. Variability in the western equatorial Pacific Ocean during the 1986–87 El Niño/Southern Oscillation event. *Journal of Physical Oceanography, 20*(2), 190–208 (1990).

We describe variability in the western Pacific Ocean during the 1986–87 El Niño/Southern Oscillation (ENSO) event, with emphasis on time series measurements of currents, temperature, sea level and winds near the equator at 165°E. Zonal winds were anomalously westerly from mid-1986 to late 1987 and were punctuated by 2–10 m s^{-1} episodes of westerlies lasting about 10 days to 2 months. Zonal currents in the upper 100-m surface layer responded to these wind variations typically within a week, in some cases with speeds exceeding 100 cm s^{-1} to the east. Zonal current variations in the thermocline below 100 m were generally less coherent with the local winds than currents near the surface. They were also generally less variable, although the Equatorial Undercurrent disappeared for 3–4 weeks in October-November 1987 at a time when the normal eastward directed zonal pressure gradient force reversed along the equator. Periods of intense and prolonged eastward flow in the surface layer were associated with a decrease in sea level by 10–20 cm at the end of 1986 and in May-August, 1987. Similarly, significant westward flow near the surface and in the thermocline in September-November 1987 was accompanied by rising sea level and a westward migration from the date line of surface waters >30°C. These results suggest that

wind-driven zonal currents at the equator were important in the evolution of the mass and heat balance of the western Pacific during the 1986–87 ENSO. Conversely, meridional wind stress and meridional velocity energy levels at periods longer than 100 days on the equator were 5–10 times weaker than in the zonal direction and less obviously related to the evolution of the 1986–87 ENSO.

MCPHADEN, M.J., H.B. MILBURN, A.I. NAKAMURA, and A.J. SHEPHERD. PROTEUS—Profile Telemetry of Upper Ocean Currents. Proceedings MTS '90, Marine Technology Society, Washington, D.C., 353–357 (1990).

In this paper we describe the development of a real-time capability for satellite transmission of acoustic Doppler current profiler (ADCP) data from deep water surface moorings. This development, which we call PROTEUS (PROfile TElemetry of Upper ocean currentS), consists of a downward-looking, surface buoy-mounted 153.6 kHz RDI ADCP with an Argos satellite telemetry link. Our efforts have been motivated by a need for real-time velocity profiles in support of short-term climate studies of El Niño and the Southern Oscillation. The first PROTEUS mooring was successfully deployed in April 1990 at 0°, 140°W as part of NOAA's EPOCS program. We describe the mooring configuration, the Argos data format, and the velocity data itself from the first 6 weeks of deployment. We also present a preliminary intercomparison of PROTEUS data from the first depth bin below the surface with data collected in real-time from a Vector Measuring Current Meter moored 17 km to the east of the PROTEUS mooring.

MCPHADEN, M.J., and P. Ripa. Wave-mean flow interactions in the equatorial ocean. *Annual Reviews of Fluid Mechanics, 22*, 167–205 (1990).

No abstract.

MILBURN, H.B., and E.N. BERNARD. Deep ocean tsunami observations. Proceedings, IRIS/JOI Workshop on Scientific Uses of Undersea Cables, A.D. Chave, R. Butler, and T.E. Pyle (eds.), Honolulu, HI, Jan. 30–Feb. 1, 1990, 69–73 (1990).

No abstract.

Mobley, C.D. A numerical model for the computation of radiance distributions in natural waters with wind-roughened surfaces. *Limnology and Oceanography, 34*(8), 1473–1483 (1989).

A numerical technique is presented for computing radiance distributions in natural waters that have wind-blown surfaces and depth-dependent inherent optical properties. Input to the numerical model consists of the radiance distribution incident on the air-water surface from above, the wind velocity, which specifies the state of randomness of the air-water surface via a wind speed-wave slope spectrum, the volume scattering and volume attenuation functions of the water body as functions of depth and wavelength, and the type of bottom

boundary. Primary output from the model consists of directionally discretized radiances as functions of wavelength, direction, and depth throughout and above the water body.

MOFJELD, H.O. Long-term trends and interannual variations of sea level in the Pacific northwestern region of the United States. Oceans '89 Proceedings, Seattle, WA, September 18–21, 1989, Vol. 1: Fisheries, Global Ocean Studies, Marine Policy and Education, Oceanographic Studies. Marine Technology Society, IEEE Publication Number 89CH2780-5, 228–230 (1989).

Long-term observations of sea level at sites in the inland and coastal waters of Washington State provide a useful case study of how sea level trends relative to the land can vary in magnitude and even in sign within the same geographical region. Within 200 km, increases in relative sea level occur at Seattle (1.9 mm/yr) in Puget Sound and Friday Harbor (1.0 mm/yr) to the north, while a decrease occurs at Neah Bay (–1.6 mm/yr) near the coast. These trends are comparable in magnitude with the average (1.5 mm/yr) for the coast of the United States. Tectonic processes seem to account for the variations in trend. The smaller trend at Friday Harbor is consistent with more intense glacial rebound due to heavier ice loading during the last ice age, while decreasing relative sea level at Neah Bay is consistent with uplift due to subduction of the Juan de Fuca Plate under the North American Plate. Superimposed on the trends are interannual variations in sea level associated with El Niño events (e.g., 1914–15, 1940–41 and 1982–83) in which higher oceanic temperatures increased sea level (up to 30 cm for the 1982–83 winter period). Interannual variations in atmospheric pressure and wind forcing also cause large variations in sea level from year to year, predominantly in winter.

NAKAMURA, A.I., R. NEWMAN, and H.B. MILBURN. Florida current cross-stream voltage measurement methodology and instrumentation. Oceans '89 Proceedings, Seattle, WA, September 18–21, 1989, Vol. 5: Diving Safety and Physiology, Ocean Engineering/Technology. Marine Technology Society, IEEE Publication Number 89CH2780-5, 1584–1587 (1989).

No abstract.

OVERLAND, J.E. Prediction of vessel icing for near-freezing sea temperatures. *Weather and Forecasting, 5*(1), 62–77 (1990).

The operational NOAA categorical vessel icing algorithm is evaluated with regard to advances in understanding of the icing process and forecasting experience. When sea temperatures are <2–3°C above the saltwater freezing point there is the likelihood of supercooling of the spray during its trajectory and extreme ice accretion on topside structures. The NOAA algorithm shows excellent results when compared to a new cold-water dataset from the Labrador Sea (mean sea temperature of –1.3°C), even though the algorithm was developed from an Alaskan dataset with a mean sea temperature of 3.6°C. A rederived algorithm from the combined data set is nearly identical to the operational algorithm. The influence of sea temperature in the NOAA model is consistent with the supercooling hypothesis and an additional icing category of extreme is recommended for the algorithm.

Severe icing in the Bering Sea, Gulf of Alaska, and Sea of Japan is primarily caused by extreme cold-air advection, while low sea temperatures contribute to severe icing in the Labrador Sea, Denmark Strait, and Barents Sea. Indirect verification showed that NOAA provided excellent forecasts to over 140 fishing vessels in Alaskan waters during late January 1989, the worst icing episode of the decade. This case suggests that current-generation atmospheric models are capable of providing reliable 36-h forecasts of cold-air advection, and thus indicating regions of heavy icing. A wave height/wind speed threshold for the onset of topside icing is 5 m s^{-1} for a 15-m vessel, 10 m s^{-1} for a 50-m trawler and 15 m s^{-1} for a 100-m vessel, developed from seakeeping theory. These wind speeds are exceeded 83%, 47% and 15%, respectively, during February in the Bering Sea.

PAULSON, A.J., M.M. Benjamin, and J.F. Ferguson. Zn solubility in low carbonate solutions. *Water Research,* 23(12), 1563–1569 (1989).

While the importance of several metal basic carbonates has been recognized in natural and wastewater systems, the existence of the Zn basic carbonate, hydrozincite, has not been fully appreciated even though solubility data have been available. In the presence of 2 mM total inorganic carbonate, Zn^{2+} solutions below pH 8.2 were found to precipitate hydrozincite within 24 h and to contain total dissolved Zn concentrations that were comparable to those predicted from equilibrium with hydrozincite. The identity of the hydrozincite was confirmed by X-ray diffraction and elemental analyses. In the pH range 8.2–10.5, the total dissolved Zn concentrations were less than that expected from equilibrium with hydrozincite by factors of up to 3, while the precipitated solids had C:Zn ratios intermediate between those of hydrozincite and give oxide and exhibited weak hydrozincite X-ray diffraction patterns. At pHs above 10.5, zinc oxides with strong X-ray diffraction patterns were present and total dissolved Zn concentrations approached those expected for equilibrium with zinc oxide. In solutions prepared to exclude carbonate, the total dissolved zinc concentrations in all solutions were similar to those expected for equilibrium with zinc oxide. However, two solids in these "carbonate-free" solutions contained small amounts of inorganic carbonate and exhibited weak hydrozincite X-ray diffraction patterns. The presence of well-defined or poorly-crystalline hydrozincite in all 2 mM inorganic carbon solutions between pH 8–10 and its presence in two solutions prepared to exclude carbonate contamination suggest that hydrozincite is probably a common Zn solid formed in conventional precipitation processes.

PAULSON, A.J., H.C. CURL, JR., and R.A. FEELY. Estimates of trace metal inputs from non-point sources discharged into estuaries. *Marine Pollution Bulletin,* 20(11), 549–555 (1989).

Elliott Bay and Duwamish Waterway, Washington were sampled for dissolved trace metals during a period of wet weather in January 1986. High concentrations of dissolved Cu, Zn, Pb, Cd and less elevated concentrations of dissolved Ni were found in marine waters adjacent to operating shipyards and a combined sewer overflow pipe that was discharging. Changes in the transports of dissolved trace metals, which have been deduced from trace metal-salinity plots, were attributed to emissions from anthropogenic sources. While 65% of the dissolved Cu and Zn transported from Elliott Bay were attributed to emissions from shipyards along Elliott Bay's shoreline, an additional 30% of the Zn was added by industrial areas adjacent

to waterways supplying freshwater. Only 20% of the Elliott Bay dissolved Ni transport was contributed by shoreline sources. In contrast, anthropogenic sources did not increase the transport of dissolved Fe.

PEASE, C.H., and P. TURET. Sea ice drift and deformation in the western Arctic. Oceans '89 Proceedings, Seattle, WA, September 18–21, 1989, Vol. 4: Acoustics, Arctic Studies. Marine Technology Society, IEEE Publication Number 89CH2780-5, 1276–1281 (1989).

Groups of ARGOS sea ice buoys were deployed in the Bering, Chukchi, and Beaufort seas over a decade. The pattern that emerges shows that Norton Sound and the coastal zone of the Seward Peninsula episodically produce ice that is both exported to the Arctic through Bering Strait and fed to the conveyor belt system of the southern Bering Sea. Additional major ice formation centers for the Bering system are the west coast of Alaska from the Yukon to Nunivak Island during easterly winds and the St. Lawrence Island polynya and Chukotsk Peninsula during northerly winds. Additional ice formation centers for the Chukchi system are the west coast of Alaska during easterly winds and intrusions of ice from the Beaufort coastal zone. There is a net partitioning of the drift in the Chukchi between the Alaskan Coastal Current and the broad flow out Hope Valley toward Wrangel Island. Although the vector mean drift in Bering Strait is northward, the mean is smaller than the currents at depth because of wind reversals and the interannual variability is large. Mesoscale strain was estimated for triplets of ARGOS buoy tracks in the western Arctic. On the open Bering Shelf tidal energy dominates both the velocity field (20–50%) and the components of the strain field. Also the M_4 tidal component of the ice velocity is about 45% of the amplitude of M_4, while M_4 in the ocean current is about 2%. This partial shift from semi-diurnal (12.4-hr) to 6.2-hour energy is caused by a compressional wave which propagates through the pack at both extremes of the semi-diurnal tidal oscillation. Daily gaps in the ARGOS coverage due to the distribution of satellite passes at low polar latitudes can be bridged best by using the tidal information from regional current measurements with appropriately enhanced M_4 to help generate a synthetic series, rather than least-squares or spline curve fitting techniques.

Perillo, G.M.E., and J.W. LAVELLE. Sediment transport processes in estuaries: An introduction. *Journal of Geophysical Research, 94*(C10), 14,287–14,288 (1989).

No abstract.

Picaut, J., A.J. Busalacchi, M.J. MCPHADEN, and B. Camusat. Validation of the geostrophic method for estimating zonal currents at the equator from Geosat altimeter data. *Journal of Geophysical Research, 95*(C3), 3015–3024 (1990).

The applicability of satellite altimeter data for estimating zonal current variability at the equator is assessed using the meridionally differenced form of the geostrophic balance. Estimates of geostrophic zonal flow anomalies in the equatorial Pacific have been deduced from 17-day collinear altimeter data during the first year of the Geosat Exact Repeat Mission,

November 1986 to November 1987. Altimeter-derived geostrophic estimates agree well with in situ zonal current variability. Comparison of low-frequency, near-surface zonal current observed from equatorial moorings at 165°E, 140°W, and 110°W yield correlations of 0.83, 0.85, and 0.51, respectively, with a mean rms difference of 23 cm s^{-1}. The geostrophic currents were calculated from all available ascending and descending Geosat tracks within ±4.5° of longitude from each mooring site. The inclusion of up to 11 ascending and descending Geosat tracks within the 9° band for every 17-day repeat effectively reduced the temporal sampling interval to 1.5 days at 165°E and 140°W. However, only ascending tracks were available at 110°W. Alongtrack sea surface heights were first smoothed using a combination of linear and nonlinear filters. The 6.8 km alongtrack spacing of the altimeter measurements provides sufficient resolution for the effective filtering of small-scale meridional noise, both instrumental and oceanic. High-frequency temporal variability, such as noise and ageostrophic motions, was suppressed with a 31-day Hanning filter. Sea level and zonal velocity solutions from a tropical Pacific numerical model were used as proxy data sets in order to estimate errors induced into the geostrophic calculation by the Geosat space-time sampling.

Picaut, J., B. Camusat, T. Delcroix, M.J. MCPHADEN, and A.J. Busalacchi. Surface equatorial flow anomalies in the Pacific Ocean during the 1986–87 ENSO using GOESAT altimeter data. Proceedings of the Western Pacific International Meeting and Workshop on TOGA COARE, Nouméa, New Caledonia, May 24–30, 1989. ORSTOM, 301–309 (1989).

Estimates of surface geostrophic zonal flow in the equatorial Pacific are deduced from the 17-day exact repeat orbit GEOSAT measurements for the period November 1986–November 1987. This period coincides with the height of the 1986–87 ENSO. Along-track altimeter height anomalies are first smoothed using a combination of linear and nonlinear filters. By combining several tracks in the zonal direction and filtering in time, we are able to obtain low frequency sea surface height at any point of the tropical Pacific. Currents are calculated from the differentiated form of the meridional momentum equation at the equator and from the classical first derivative of the meridional pressure field away from the equator. Comparisons of low frequency near-surface zonal current directly measured from equatorial moorings at 165°E, 140°W and 110°W yield a correlation of 0.83, 0.84, and 0.50 respectively with a mean rms difference of 0.23 m s^{-1}. Sea level and zonal velocity solutions from a tropical Pacific numerical model are used as proxy data sets in order to quantify errors induced to quantify the geostrophic calculation by the GEOSAT space-time sampling. In December 1986, a downwelling equatorial Kelvin wave is generated in the western Pacific and shows up, near the forcing area, as an intense local 1 m s^{-1} eastward equatorial surface flow anomaly. This Kelvin wave propagates into the eastern equatorial Pacific with a phase speed of about 2.5 m s^{-1} and is associated with eastward equatorial current anomalies of 0.3–0.5 m s^{-1}. In February 1987, an upwelling equatorial Kelvin wave is excited near the date line and propagates eastward. This wave, characterized by a westward flow anomaly of 0.3–0.8 m s^{-1}, reaches the eastern Pacific boundary in March 1987 where it forces apparently an upwelling first meridional mode equatorial Rossby wave. This Rossby wave propagates westward in the ocean interior at about 0.8 m s^{-1} as a patch of equatorially trapped eastward flow (0.6–0.8 m s^{-1} maximum) flanked, in both hemispheres, by 0.2–0.4 m s^{-1} westward flow anomalies which decreased the South Equatorial Current and the North and South Equatorial

Countercurrents. The equatorial Rossby wave propagation could be traced sequentially through the eastern, central and western Pacific from April to September 1987. Thus GEOSAT altimeter data indicate that equatorial Kelvin waves and possible eastern reflection as equatorial Rossby waves are an important component of basin scale surface current variability during the 1986–87 ENSO.

PROCTOR, P.D. Fisheries-Oceanography Coordinated Investigations—Field Operations 1988. NOAA DR ERL PMEL-25 (NTIS PB90-159088), 69 pp. (1989).

No abstract.

QUINN, P.K., T.S. BATES, J.E. JOHNSON, D.S. Covert, and R.J. Charlson. Interactions between the sulfur and reduced nitrogen cycles over the central Pacific Ocean. *Journal of Geophysical Research, 95*(D10), 16,405–16,416 (1990).

In April and May of 1988 along 170°W from 53°N to 14°S, simultaneous concentration measurements were made of the major components of the sulfur and reduced nitrogen cycles. The species measured included seawater dimethylsulfide, DMS (s), and total ammonia, NH_3 (s,tot) = NH_3 (s) + NH_4^+ (s); atmospheric gas phase DMS (g), NH_3 (g), and SO_2 (g); and atmospheric particulate phase NH_4^+ (p), non-seasalt sulfate, nss $SO_4^=$ (p), and methanesulfonate, MSA (p). Based on isentropic calculated back trajectories at 1000, 950, 850, and 700 mbar arrival heights, three apparent air mass regimes were encountered; one from 50°N to 30°N which recently had been in contact with Asia, one from 29°N to 15°N which had passed over Hawaii during a volcanic eruption several days earlier, and one from 14°N to 11°S which was the most representative of remote marine air. Changes in the relative concentrations of the atmospheric S and NH_3 species reflected the origin of the air masses sampled. The NH_3 (g) concentrations were low over the entire region studied, indicating that the lifetime of NH_3 in the marine boundary layer is on the order of hours. These low NH_3 concentrations led to only partially neutralized sulfate aerosol particles. The mean NH_4^+ (p) to nss $SO_4^=$ (p) molar ratio was 1.3 ± 0.71. The highest ratios were found in continentally influenced air masses where the NH_4^+ (p) was most likely of continental origin and in remote marine air masses with an absence of continentally derived nss $SO_4^=$ (p). The lowest ratios found were a result of high nss $SO_4^=$ (p) concentrations in air masses influenced by the Hawaiian volcanic plume. Seawater concentrations of DMS (s) and NH_3 (s,tot) were lowest in the North Pacific central gyre and highest in the northern latitudes and near and south of the equator.

REED, R.K., L.S. Incze, and J.D. SCHUMACHER. Estimation of the effects of flow on dispersion of larval pollock, *Theragra chalcogramma*, in Shelikof Strait, Alaska. Effects of ocean variability on recruitment and an evaluation of parameters used in stock assessment models, R.J. Beamish and G.A. McFarlane (eds.), Canadian Special Publication of Fisheries and Aquatic Sciences 108, 239–246 (1989).

The focus of this work is to examine the effects of oceanic motions on the larvae of walleye pollock, *Theragra chalcogramma*, in Shelikof Strait, Alaska. A baroclinic coastal current flows southwestward through Shelikof Strait with typical peak speeds of 20 cm s^{-1}. Data from current moorings were used to derive eddy diffusivities and horizontal divergence (typical estimates were 5×10^6 cm^2 s^{-1} and -1.5×10^{-6} s^{-1}, respectively). The effects of horizontal advection, divergence, and turbulent diffusion on changing concentration of larvae with time were estimated. The estimates suggest that all factors may be important. Finally, changes which could result from physical effects were compared with observed changes in abundance and distribution to estimate larval mortality.

REED, R.K., and P.J. STABENO. Circulation and property distributions in the central Bering Sea, Spring 1988. NOAA TR ERL 439-PMEL 39 (NTIS PB90-155847), 13 pp. (1989).

Data from a synoptic CTD survey in the central Bering Sea in winter 1988 are used to examine circulation and property distributions. A coherent, cyclonic circulation existed over much of the region. Geostrophic flow as great as 40 cm s^{-1} was present over the continental slope; another branch of relatively strong flow was situated over the shelf near a surface salinity front. The characteristic subsurface temperature minimum and maximum were both found in less dense water than in previous observations. Six satellite-tracked drifting buoys were also deployed. Their paths were in general agreement with the geostrophic flow, but some small eddies were revealed by the drifters that were not detected by the CTD data.

REED, R.K., and P.J. STABENO. Recent observations of variability in the path and vertical structure of the Alaskan Stream. *Journal of Physical Oceanography, 19*(10), 1634–1642 (1989).

Current records were recently obtained from two sites on the continental slope southwest of Kodiak Island. At the inshore site (10-month record), flow mainly resembled the weak shelf-break flow typical of the Gulf of Alaska. Except for two periods, each of ~3 months duration, the offshore site (31-month record) was in the path of the Alaskan Stream. During the Alaskan Stream segments, flow characteristics (low eddy energy, high vertical coherence, and high stability) were similar to those in the stream at other locations. When the stream was absent from the offshore site, it made a seaward excursion of ~50 km as evidenced by satellite-tracked drifters. The cause of this migration is unclear. During a period of ~6 months, a subsurface velocity maximum was measured at 165 m. Flow near 1000 m was very weak for almost two years; geostrophic flow estimates, however, suggest this is a rare situation.

Savage, D.S. Fisheries-Oceanography Coordinated Investigations—Field Operations 1989. NOAA DR ERL PMEL-26 (NTIS PB90-208448), 68 pp. (1990).

No abstract.

SCHUMACHER, J.D., and A.W. Kendall, Jr. Fisheries Oceanography Coordinated Investigations (FOCI): Walleye pollock recruitment in the western Gulf of Alaska. Proceedings of the Gulf of Alaska, Cook Inlet, and North Aleutian Basin Information Update Meeting, Anchorage, AK. OCSEAP/MMS, 39–47 (1989).

No abstract.

SCHUMACHER, J.D., P.J. STABENO, and A.T. ROACH. Volume transport in the Alaska Coastal Current. *Continental Shelf Research, 9*(12), 1071–1083 (1989).

Nine moorings were deployed in three sections in the Shelikof Strait/Semidi Islands region of the Alaskan continental shelf during the period of August 1984 to July 1985. Analysis of the resulting current and bottom pressure data, together with surface wind, provides a new understanding of transport in the Alaska Coastal Current. Using current observations, mean volume transport through the Shelikof sea valley was computed to be 0.85×10^6 m^3 s^{-1}, which is in good agreement with estimates of transport obtained from hydrographic data. Approximately 75% of this flux flowed seaward through the Shelikof sea valley, with the remainder flowing along the Alaska Peninsula. Data showed the expected increase of volume transport concomitant with maximum freshwater discharge in autumn. The greatest monthly mean transport, however, occurred in winter and was related to wind forcing. On time intervals of days, fluctuations in transport were often large (up to 3.0×10^6 m^3 s^{-1}), and generally geostrophic ($r = 0.79$). Some of these fluctuations resulted from convergence of flow caused by the complex interaction of storms with orography. Approximately half of the fluctuations in volume transport were accounted for by the alongshore wind.

Smith, S.D., R.D. Muench, and C.H. PEASE. Polynyas and leads: An overview of physical processes and environment. *Journal of Geophysical Research, 95*(C6), 9461–9479 (1990).

Polynyas and leads are openings in pack ice due to divergences in ice drift and to local melting. They are the vents and windows to the polar oceans. In winter they are a major source of brine during freezing and a locus for gas exchange. Large sensible heat fluxes, together with evaporation and longwave radiation from a very small percentage of open water and thin ice, dominate regional heat budgets. In summer, solar radiation is absorbed by open water but is reflected from snow-covered pack ice. Experiments and models describing these processes are reviewed.

JISAO PUBLICATIONS

Arlander, D.W., D.R. Crown, J.C. Farmer, F.A. Menzia, and H.H. Westerberg (1990): Gaseous oxygenated hydrocarbons in the remote marine troposphere. *J. Geophys. Res., 95*(D10), 16,391–16,403.

Battisti, D.S., A. Hirst, and E.S. Sarachik (1989): Instability and predictability in coupled atmosphere-ocean models. *Trans. Roy. Soc. London, A329*, 237–247.

Butterfield, D.A., G.J. Massoth, R.E. McDuff, J.E. Lupton, M.D. Lilley, and I.R. Jonasson (1989): Submarine venting of phase separated hydrothermal fluids at Axial Volcano, Juan de Fuca Ridge. *Nature, 340*, 702–705.

Chang, P. (1990): Oceanic adjustment in the presence of mean currents on an equatorial B-plane. *J. Geophys. Res., 95*(C9), 15,975–15,995.

Chang, P. (1990): Quasigeostrophic oceanic adjustment in the presence of mean currents. *Dynamics of Atmosphere and Oceans, 14*, 387–414.

Davison, J. and D.E. Harrison (1990): Comparison of SEASAT scatterometer winds with tropical Pacific observations. *J. Geophys. Res., 95*(C3), 3403–3410.

Giese, B.S. and D.E. Harrison (1990): Aspects of the Kelvin wave response to episodic wind forcing. *J. Geophys. Res., 95*(C5), 7289–7312.

Haynes, P.H. (1989): The effect of barotropic instability on the non-linear evolution of a Rossby-wave critical layer. *J. Fluid Mech., 207*, 231–266.

Harrison, D.E., B.S. Giese and E.S. Sarachik (1990): Mechanisms of SST change in the equatorial waveguide during the 1982–83 ENSO. *J. Climate, 3*, 173–188.

Johnson, J.E., R.H. Gammon, J. Larsen, T.S. Bates, S.J. Oltmans and J.C. Farmer (1989): Ozone in the marine boundary layer over the Pacific and Indian Oceans: Latitudinal gradients and diurnal cycles. *J. Geophys. Res., 95*(D8), 11,847–11,856.

Kessler, W.S. (1990): Observations of long Rossby waves in the northern tropical Pacific. *J. Geophys. Res., 95*(C4), 5183–5217.

Landsteiner, M.C., M.J. McPhaden and J. Picaut (1990): On the sensitivity of Sverdrup transport estimates to the specification of wind stress forcing in the tropical Pacific. *J. Geophys. Res., 95*(C2), 1681–1691.

McPhaden, M.J. and P. Ripa (1990): Wave-mean flow interactions in the equatorial ocean. *Ann. Rev. Fluid Mech., 22*, 167–205.

Mobley, C.D. (1989): A numerical model for the computation of radiance distributions in natural waters with wind-roughened surfaces. *Limnol. Oceanogr., 34*(8), 1473–1483.

Nakamura, N., and I.M. Held (1989): Nonlinear equilibration of two-dimensional eddy waves. *J. Atmos. Sci., 46*(19), 3055–3064.

Sarachik, E.S. (1990): Predictability of ENSO. Ocean Climate Interactions, 161–171.

Sarachik, E.S., and R.H. Gammon (1989): The role of the ocean in the NOAA Program, "Climate and Global Change." NOAA Climate and Global Change Program, Special Report No. 1, 1–31.

Wakata, Y., and Y. Sugimori (1990): Lagrangian motions and global density distributions of floating matter in the ocean simulated using shipdrift data. *J. Phys. Oceanogr., 20*(1), 125–138.

Weaver, A., and J.H. Middleton (1990): An analytic model for the Leeuwin Current off western Australia. *Cont. Shelf Res., 10*(2), 105–122.

Weaver, A., and E.S. Saracnik (1990): On the importance of vertical resolution in certain ocean general circulation models. *J. Phys. Oceanogr., 20*, 600–609.

JIMAR PUBLICATIONS

Bahr, F., E. Firing, and S.N. Jiang (1989): Acoustic Doppler current profiling in the western Pacific during the US-PRC TOGA cruises 2, 3, and 4. JIMAR Data Report 005.

Bahr, F., E. Firing, and S.N. Jiang (1990): Acoustic Doppler current profiling in the western Pacific during the US-PRC cruises 5 and 6. JIMAR Data Report 007.

Boehlert, G.W. (1989): Biological productivity at seamounts and fisheries potential. *Proceedings, 9th Week of Fisheries of the Azores.*

Boehlert, G.W. (1989): Book review: "Marine Populations: An Essay on Population Biology and Speciation" by Michael Sinclair. *Limnol. Oceanogr., 34,* 968–969.

Busalacchi, A.J., M.J. McPhaden, J. Picaut, and S. Springer (1989): Uncertainties in tropical Pacific Ocean simulations: The seasonal and interannual sea level response to three analyses of the surface wind field. *Proceedings, TOGA-COARE Workshop,* Nouméa, New Caledonia, May 24–30, 1989, 367–378.

Busalacchi, A.J., M.J. McPhaden, J. Picaut, and S. Springer (1990): Sensitivity of wind-driven tropical Pacific Ocean simulations on seasonal and interannual time-scales. In: *Coupled Ocean-Atmosphere Models,* J.C. Nihoul (ed.), 119–154.

Chiswell, S.M., and R. Lukas (1990): Reply to "Comment on Rossby-gravity waves in central equatorial Pacific during the NORPAX Hawaii-to-Tahiti Shuttle Experiment." *J. Geophys. Res., 95*(C1), 807.

Freitag, H.P., M.J. McPhaden, and A.J. Shepherd (1989): Real-time surface currents from moored buoys. *Proceedings, North American Argos User's Conference,* May 15–17, 1989, 85–100.

Hacker, P., E. Firing, R. Lukas, P.L. Richardson, and C.A. Collins (1989): Observations of the low-latitude western boundary circulation in the Pacific during WEPOCS III. In: *Proceedings, Western Pacific International Meeting and Workshop on TOGA-COARE,* Nouméa, New Caledonia, May 24–30, 135–143.

Hayes, S.P., M.J. McPhaden, and J.M. Wallace (1989): The influence of sea surface temperature upon surface wind in the eastern equatorial Pacific: weekly-to-monthly variability. *J. Clim., 2,* 1500–1506.

Landsteiner, M., M.J. McPhaden, and J. Picaut (1990): On the sensitivity of Sverdrup transport estimates to the specification of wind stress forcing in the tropical Pacific. *J. Geophys. Res., 95,* 1681–1692.

Latif, M., J. Biercamp, H. von Storch, M.J. McPhaden, and E. Kirk (1990): Analyses of tropical anomalies simulated by an AGCM. *J. Clim., 3,* 509–521.

Lukas, R. (1989): The thermohaline structure of the western equatorial Pacific upper ocean. In: *Proceedings, International Symposium on Japanese Pacific Climate Study (JAPACS)*, Tsukuba Science City, Japan, Oct. 19–20, 1989, 231–232.

Lukas, R. (1989): Observations of air-sea interactions in the western Pacific warm pool during WEPOCS. In: *Proceedings, Western Pacific International Meeting and Workshop on TOGA-COARE*, Nouméa, New Caledonia, May 24–30, 1989, 599–610.

Lukas, R., W. Patzert, G. Meyers, and W. Emery (1990): Klaus Wyrtki's forty years of contributions to oceanography: His students' perspective. *Oceanogr., 3*, 36–38.

Maliekal, J.A., M.A. Lander, and M.L. Morrissey (1989): Comparison of the zonal propagation of equatorial OLR fields during the three recent El Niños. *Proceedings, 14th Annual Climate Diagnostics Workshop*, San Diego, California, Oct. 16–20, 1989.

Mangum, L.J., S.P. Hayes, J.M. Toole, Z. Wang, S. Pu, and D. Hu (1989): Thermohaline structure and zonal pressure gradient in the western equatorial Pacific. *J. Geophys. Res., 95*, 7279–7288.

McPhaden, M.J. (1990): Comment on Chiswell and Lukas, "Rossby-gravity waves in the central equatorial Pacific during the NORPAX Hawaii-to-Tahiti Shuttle Experiment." *J. Geophys. Res., 95*, 805–806.

McPhaden, M.J., S.P. Hayes, L.J. Mangum, and J. Toole (1990): Variability in the western equatorial Pacific during the 1986–87 El Niño/Southern Oscillation event. *J. Phys. Oceanogr., 20*, 190–208.

Meir, M., H.R. Buckley, and J.J. Polovina (1989); A debate on responsible artificial reef development. *Bull Mar. Sci., 44*(2), 1051–1057.

Moffitt, R.B., F.A. Parrish, and J.J. Polovina (1989): Community structure, biomass, and productivity of deepwater artificial reefs in Hawaii. *Bull. Mar. Sci., 44*(2), 616–630.

Morrissey, M.L. (1990): An evaluation of ship data in the equatorial Western Pacific. *J. Clim., 3*, 99–112.

Morrissey, M.L., and J.S. Greene (1989): Verification of satellite-based rainfall estimates for climate models. *Proceedings, 14th Annual Climate Diagnostics Workshop*, San Diego, California, Oct. 16–20, 1989.

Picaut, J., A.J. Busalacchi, M.J. McPhaden, and B. Camusat (1990): Validation of the geostrophic method for estimating zonal currents at the equator from GEOSAT altimeter data. *J. Geophys. Res., 95*, 1681–1692.

Picaut, J., B. Camusat, T. Delcroix, M.J. McPhaden, and A.J. Busalacchi (1989): Surface equatorial flow anomalies in the Pacific Ocean during the 1986–87 ENSO using GEOSAT altimeter data. *Proceedings, TOGA-COARE Workshop*, Nouméa, New Caledonia, May 24–30, 1989, 301–312.

Polovina, J.J. (1989): Artificial reefs: Nothing more than benthic fish aggregators. *Proceedings, Calif. Coop. Oceanic Fish. Invest.*

Polovina, J.J. (1989): Density dependency in spiny lobster, *Panulirus marginatus*, in the northwestern Hawaiian Islands. *Can. J. Fish. Aquat. Sci., 46*(4), 660–665.

Polovina, J.J. (1989): A system of simultaneous dynamic production equations: Application to fishery forecasting in an island archipelago. *1988 AFS Annual Meeting.*

Polovina, J.J. (1990): Application of yield-per-recruit and surplus production models to fishery enhancement through juvenile releases. *Proceedings, 12th U.S.-Japan Panel Meeting on Aquaculture, Symposium on Marine Ranching*, Kyoto, Japan, Oct. 19–29, 1986.

Polovina, J.J. (1990): Modeling fish stocks: Applicability, problems, and requirements for multispecies and multigear fisheries in the tropics. *FAO Technical Report*, 41 pp.

Polovina, J.J., and I. Sakai (1989): Impacts of artificial reefs on fishery production in Shimamaki, Japan. *Bull. Mar. Sci., 44*(2), 997–1003.

Rui, H., and B. Wang (1990): Development characteristics and dynamic structure of tropical intraseasonal convection anomalies. *J. Atmos. Sci., 47*, 357–379.

Seaman, W., Jr., R.M. Buckley, and J.J. Polovina (1989): Advances in knowledge and priorities for research, technology and management related to artificial aquatic habitats. *Bull. Mar. Sci., 44*(2), 527–532.

Tsuchiya, M., R. Lukas, R.A. Fine, E. Firing, and E. Lindstrom (1989): Source waters of the Pacific Equatorial Undercurrent. *Prog. Oceanogr., 23*, 101–147.

Wang, B., and J. Chen (1989): On the zonal scale selection and vertical structure of the equatorial intraseasonal waves. *Q. J. Roy. Met. Soc., 115*, 1301–1323.

Wang, B., and H. Rui (1990): Dynamics of the coupled moist Kelvin-Rossby wave on an equatorial B-plane. *J. Atmos. Sci., 47*, 397–413.

Wilson, C.D., and G.W. Boehlert (1990): Acoustic measurement of micronekton distribution over Southeast Hancock Seamount, Central Pacific Ocean. In: *Acoustic Remote Sensing, Proceedings, Fifth International Symposium on Acoustic Remote Sensing of the Atmosphere and Oceans*, S.P. Singal (ed.), 222–229.

Wyrtki, K. (1990): Sea level rise: The facts and the future. *Pac. Sci., 44*, 1–16.

Wyrtki, K., and G.T. Mitchum (1990): Interannual differences of GEOSAT altimeter heights and tide gauge data: The importance of a datum. *J. Geophys. Res., 95*, 2969–2975.

CIMRS PUBLICATIONS

Appelgate, T.B. (1990): Volcanic and structural morphology of the south flank of Axial Volcano, Juan de Fuca Ridge: Results from a Sea MARC I sidescan sonar survey. *J. Geophys. Res., 95*(B8), 12,765–12,783.

Embley, R.R., K.M. Murphy, and C.G. Fox (1990): High resolution studies of the summit of Axial Volcano. *J. Geophys. Res., 95*(B8), 12,785–12,812.

Fox, C.G., F.J. Jones, and T.K. Lau (1990): Enhanced imagery from Sea MARC I sidescan sonar. Special Issue on Bathymetry and Seafloor Acoustic Remote Sensing, *IEEE J. Oceanic Eng., 15*(1), 24–31.

GLOSSARY OF ACRONYMS

A&P:	Analysis and Prediction [program] (FSL)
AAOE:	Airborne Antarctic Ozone Experiment
AASE:	Airborne Arctic Stratospheric Experiment
ACC:	Alaska Coastal Current
ACCP:	Atlantic Climate Change Program
ADCP:	Acoustic Doppler Current Profiler
ADIOS:	Asian Dust Input to the Oceanic System
AFTAD:	Analysis-Forecast Transport and Diffusion
AGASP:	Arctic Gas and Aerosol Sampling Program
AI:	Artificial intelligence
AID:	Agency for International Development
AL:	Aeronomy Laboratory (ERL)
AOML:	Atlantic Oceanographic and Meteorological Laboratory (ERL)
APEX:	Arctic Polynya Experiment
APL:	Applied Physics Laboratory
ARGOS:	French satellite used to telemeter data to shore stations (not an acronym)
ARL:	Air Resources Laboratory (ERL)
ASCOT:	Atmospheric Studies in Complex Terrain (DOE)
ASG:	Administrative Support Group (PMEL)
ASHES:	Axial Seamount Hydrothermal Emissions Study
ATLAS:	Automated Temperature Line Acquisition System
AVHRR:	Advanced Very-High-Resolution Radiometer
AVIRIS:	Airborne Visible and Infrared Imaging Spectrometer
AWIPS-90:	Advanced Weather Interactive Processing System for the 1990s
AXBT:	Airborne XBT
AXCP:	Airborne Expendable Current Profiler
BLIPS:	Benthic Layer Interactive Profiling System
BMRC:	Bureau of Meteorology Research Center
BPR:	Bottom Pressure Recorder
BT:	Bathythermograph
CAPS:	Center for Analysis and Prediction of Storms
CARD:	Coastal and Arctic Research Division [formerly MSRD] (PMEL)
CASE:	Coordinated Air-Sea Experiment
CCCO:	Committee on Climate Changes and the Ocean
CCIW:	Canada Centre for Inland Waters
CCOPE:	Cooperative Convective Precipitation Experiment
CCRS:	Canada Centre for Remote Sensing
CEAREX:	Coordinated Eastern Arctic Experiment
CFC:	Chlorofluorocarbon
CFM:	Chlorofluoromethane
CG:	Cloud to Ground
CGC:	Climate and Global Change
CILER:	Cooperative Institute for Limnology and Ecosystems Research
CIMAS:	Cooperative Institute for Marine and Atmospheric Studies
CIMMS:	Cooperative Institute for Mesoscale Meteorological Studies
CIMRS:	Cooperative Institute for Marine Resources Studies
CIRA:	Cooperative Institute for Research in the Atmosphere
CIRES:	Cooperative Institute for Research in Environment Sciences
CITE-3:	Chemical Instrumentation and Test Evaluation (NASA)
CLASS:	Cross-chain LORAN Atmospheric Sounding System

CLICOM:	Climate Computing
CMDL:	Climate Monitoring and Diagnostics Laboratory
CME:	Coronal Mass Ejection
CNES:	Centre Nationale d'Etudes Spatiales
CNSD:	Computer and Network Support Division [formerly CSG] (PMEL)
COADS:	Comprehensive Ocean-Atmosphere Data Set
COAP:	Center for Ocean Analysis and Prediction (Monterey)
COARE:	Coupled Ocean-Atmosphere Response Experiment
COPS:	Cooperative Oklahoma P-3 Studies
CPUE:	Catch Per Unit [fish] Effort
CRF:	Cloud Radiation Feedback
CRREL:	Cold Regions Research and Engineering Laboratory
CSES:	Center for the Study of Earth from Space
CSG:	Computer Support Group
CSIRO:	Commonwealth Scientific and Industrial Research Organization (Australia)
CSU:	Colorado State University
CTD:	Conductivity, Temperature, Depth
CVS:	Cathodic Voltametry Stripping
CZCS:	Coastal Zone Color Scanner
DARE-II:	PROFS meteorological workstation (not an acronym)
DMS:	Dimethylsulfide
DMSP:	Defense Meteorological Satellite Program
DOD:	Department of Defense
DOE:	Department of Energy
DWBC:	Deep Western Boundary Current
D.U.:	Dobson Unit
E-BPR:	Enhanced Bottom Pressure Recorder
EDD:	Engineering Development Division (PMEL)
ENSO:	El Niño-Southern Oscillation
EOF:	Empirical Orthogonal Function
EOS:	Earth Observing System (NASA)
Eos:	Eos, Transactions of the American Geophysical Union
EPA:	Environmental Protection Agency
EPIC:	Extensive PMEL Information Collection
EPOCS:	Equatorial Pacific Ocean Climate Studies
ERL:	Environmental Research Laboratories (NOAA)
FAA:	Federal Aviation Administration
FASINEX:	Frontal Air-Sea Interaction Experiment
FAST:	Flow Actuated Sediment Trap
FGGE:	First GARP Global Experiment
FIDES:	Forecaster's Intelligent Discussion Experiment System
FIFE:	First ISLSCP Field Experiment
FIRE:	First ISCCP Regional Experiment
FNOC:	Fleet Numerical Oceanography Center
FOCAL:	French Program Ocean-Climat Atlantique Equatorial
FOCI:	Fisheries-Oceanography Coordinated Investigations
FOCUS:	Fisheries Oceanography Cooperative Users System
FOX:	Fishery-Oceanography Experiment
FREEZE:	Name of arctic ice formation experiment (not an acronym)
FSL:	Forecast Systems Laboratory (ERL)
GALE:	Genesis of Atlantic Lows Experiment
GARP:	Global Atmospheric Research Program
GCM:	General Circulation Model
GEOSAT:	Geodetic Satellite
GFDL:	Geophysical Fluid Dynamics Laboratory (ERL)

GISP:	Greenland Ice Sheet Project
GISS:	Goddard Institute for Space Studies
GLERL:	Great Lakes Environmental Research Laboratory (ERL)
GLOBE:	Global Backscatter Experiment
GMC:	General Circulation Model
GMCC:	Geophysical Monitoring for Climatic Change (ARL)
GOES:	Geostationary Operational Environmental Satellite
GSFC:	Goddard Space Flight Center
GTN:	Global Trends Network
GUFMEX:	Gulf of Mexico [project]
HCFC:	Hydrochlorofluorocarbon
HIBU:	Hydrological Institute and Belgrade University
HIRIS:	High-Resolution Imaging Spectrometer
HIS:	High-Resolution Interferometer Spectrometer
HMSC:	Hatfield Marine Science Center
HOT:	Hawaiian Ocean Time series
HRD:	Hurricane Research Division (AOML)
HRPT:	High-Resolution Picture Transmission
IAMAP/IAPSO:	International Association of Meteorology and Atmospheric Physics/International Association for the Physical Sciences of the Ocean
IAMSLIC:	International Association of Marine Science Libraries & Information Centers
ICES:	International Council for the Exploration of the Sea
ICG/ITSU:	International Coordinating Group for the Tsunami Warning System in the Pacific
ICSU:	International Council of Scientific Unions
IEEE:	Institute of Electrical and Electronics Engineers
IFREMER:	Institut Français de Recherche pour l'Éxploitation de la Mer
IGBP:	International Geosphere-Biosphere Program
IGM:	Interplanetary Global Model
IGOSS:	International Global Ocean Services System
IGP:	Igneous & Geothermal Processes
IGSP:	International Greenland Sea Project
INSAT:	Indian Satellite
IOC:	International Oceanographic Commission
IPS:	Interplanetary Scintillation
IRIS:	International Recruitment Investigations in the Subarctic
IRIS:	Incorporated Research Institutions for Seismology
ISCCP:	International Satellite Cloud Climatology Project
ISEE:	International Sun-Earth Explorer
ITCZ:	Intertropical Convergence Zone
IUGG:	International Union of Geodesy and Geophysics
IUGG/TC:	IUGG Tsunami Commission
JAMSTEC:	Japan Marine Science and Technology Center
JIC:	Navy/NOAA Joint Ice Center
JIMAR:	Joint Institute for Marine and Atmospheric Research
JISAO:	Joint Institute for the Study of Atmosphere and Ocean
JOI:	Joint Oceanographic Institutions
JPL:	Jet Propulsion Laboratory
JSC:	Johnson Space Center
L-RERP:	Long-Range Effects Research Program
LAHM:	Limited Area HIBU Model
Lamont:	Lamont Doherty Geological Observatory
LAPS:	Local Analysis and Prediction System
LASCO:	Large-angle Spectrometric Coronagraph
LDGO:	Lamont Doherty Geological Observatory
LORAN:	Long-Range Aid to Navigation

MAPS:	Mesoscale Analysis and Prediction System
MARD:	Marine Assessment Research Division (PMEL)
MCLASS:	Mobile CLASS
MCS:	Mesoscale Convective System
MCV:	Mesoscale Convectively Generated Vortices
MHD:	Magnetohydrodynamic
MIT:	Massachusetts Institute of Technology
MIZ:	Marginal Ice Zone
MIZEX:	Marginal Ice Zone Experiment
MLD:	Mixed Layer Depth
MMS:	Minerals Management Service, U.S. Dept. of Interior
MOCNESS:	Multiple Opening and Closing Net Environmental Sampling System
MOU:	Memorandum of Understanding
MRAO:	Mullard Radio Astronomy Observatory
MRD:	Mesoscale Research Division (NSSL)
MRRD:	Marine Resources Research Division (PMEL)
MSRD:	Marine Services Research Division (PMEL)
MST:	Mesosphere-Stratosphere-Troposphere
mtDNA:	Metochondrial Deoxyribonucleic Acid
NADW:	North Atlantic Deep Water
NAS:	National Academy of Sciences
NASA:	National Aeronautics and Space Administration
NCAR:	National Center for Atmospheric Research
NERC:	Natural Environment Research Council
NESDIS:	National Environmental Satellite, Data, and Information Service (NOAA)
NEXRAD:	Next-Generation Weather Radar
NGDC:	National Geophysical Data Center (NOAA)
NGM:	Nested Grid Model
NHC:	National Hurricane Center (NWS)
NIC:	NOAA Information Center
NIMBUS-7:	NOAA satellite (not an acronym)
NMC:	National Meteorological Center (NOAA)
NMFS:	National Marine Fisheries Service (NOAA)
NOAA:	National Oceanic and Atmospheric Administration
NOAAPORT:	Access to NOAA real-time data base system (not an acronym)
NOARL:	National Oceanographic and Atmospheric Research Laboratory
NODC:	National Oceanographic Data Center
NORPAX:	North Pacific Experiment
NOS:	National Ocean Service (NOAA)
NOSC:	Naval Ocean Systems Center
NRC:	National Research Council
NRC:	Nuclear Regulatory Commission
NSF:	National Science Foundation
NSIDC:	National Snow and Ice Data Center
NSSL:	National Severe Storms Laboratory (ERL)
NURP:	NOAA Undersea Research Program
NUSC:	Naval Underwater Systems Center
NWAFC:	Northwest and Alaska Fisheries Center
NWP:	Numerical Weather Prediction
NWS:	National Weather Service (NOAA)
OAR:	Oceanic and Atmospheric Research
OCEAN STORMS:	A JISAO field experiment for the assessment of weather fronts (not an acronym)
OCRD:	Ocean Climate Research Division (PMEL)
OCS:	Outer Continental Shelf
OCSEAP:	Outer Continental Shelf Environmental Assessment Program

ODW:	Omega Dropwindsonde
OERD:	Ocean Environment Research Division [formely MARD and MRRD] (PMEL)
OLR:	Outgoing Longwave Radiation
ONR:	Office of Naval Research
ORSTOM:	Office de la Recherche Scientifique et Technique Outre-Mer
OSU:	Oregon State University
OU:	University of Oklahoma
PacTOP:	Pacific Tsunami Observation Program
PAH:	Polycyclic Aromatic Hydrocarbon
PCB:	Polychlorinated Biphenyl
PEGASUS:	Current velocity profiling instrument (not an acronym)
PENTAFLUX:	Fifth Flux Experiment
PEQUOD:	Pacific Equatorial Ocean Dynamics
PMEL:	Pacific Marine Environmental Laboratory (ERL)
POSEIDON:	French component of joint U.S./French TOPEX/POSEIDON sea-surface topography satellite mission (not an acronym)
POT:	Program for Operational Trajectories
POTAD:	Program for Operational Transport and Dispersion
PROFS:	Program for Regional Observing and Forecasting Services (FSL)
PROTEUS:	Profile Telemetry of Upper Ocean Currents
PSI:	Pacific Sulfur/Stratus Investigation
QBO:	Quasi-biennial Oscillation
RADM:	Regional Acid Deposition Model
RAMM:	Regional and Mesoscale Meteorology
RASS:	Radio Acoustic Sounding System
Ri:	Richardson Number, a dimensionless number related to stability of stratified flow
RITS:	Radiatively Important Trace Species
RJE:	Remote Job Entry
RSMAS:	Rosenstiel School of Marine and Atmospheric Sciences
S^3T:	Sequentially Sampling Sediment Trap
SA:	Spaced Antenna
SAFER:	Spectral Application of Finite Element Representation
SAIC:	Science Applications International Corporation
SAR:	Synthetic Aperture Radar
SAVE:	South Atlantic Ventilation Experiment
SBUV:	Solar Backscatter Ultraviolet
SCOR:	Scientific Committee on Oceanic Research
SCOPE:	Scientific Committee on Problems of the Environment
Scripps:	Scripps Institution of Oceanography
SEABEAM:	A shipboard multi-transducer swath echo sounding system
SEFC:	Southeast Fisheries Center
SEFCAR:	South and East Florida and Caribbean Recruitment
SEL:	Space Environment Laboratory (ERL)
SELDADS:	SEL Data Acquisition and Display System
SEM:	Space Environment Monitor
SESC:	Space Environment Services Center (SEL)
SHARE:	International program to develop meteorological analysis and display software for developing countries (not an acronym)
SIO:	Scripps Institution of Oceanography
SKYHI:	GFDL stratosphere GCM (not an acronym)
SLAR:	Side-Looking Airborne Radar
SLEUTH:	System for Locating Eruptive Underwater Turbidity and Hydrography
SLP:	Sea Level Pressure
SMM:	Solar Maximum Mission
SMMR:	Scanning Multichannel Microwave Radiometer

SOFAR:	Sound Fixing and Ranging (acoustical system/technique)
SSD:	Scientific Support Division (NSSL)
SSF:	Semi-Lagrangian and semi-geostrophic finite element [model]
SSM/I:	Special Sensor Microwave/Imager
SST:	Sea Surface Temperature
STACS:	Subtropical Atlantic Climate Studies
STEP:	Stratosphere-Troposphere Exchange Project
STORM:	Stormscale Operational and Research Meteorology
SXI:	Solar X-ray Imager
TAG:	Trans Atlantic Geotraverse
TAMU:	Texas A&M University
TAO:	Thermal Array for the Ocean; Tropical Atmosphere/Ocean
TASD:	Technical and Administrative Support Division (PMEL)
TDWR:	Terminal Doppler Weather Radar
TELSAR:	Tracking and Evolution of Solar Active Regions
THEO:	System for predicting solar flare probabilities, named for Theophrastus (not an acronym)
THRUST:	Tsunami Hazard Reduction Using System Technology
TIROS:	Television and Infrared Observation Satellite
TMAP:	Thermal Modeling and Analysis Project
TO-AN:	Tropical Ocean-Atmosphere Newsletter
TOGA:	Tropical Oceans and Global Atmosphere
TOPEX:	Topographic Experiment (NASA)
TOPS:	Total Ocean Profiling System
TRMM:	Tropical Rainfall Measuring Mission
TVS:	Tornado Vortex Signature
UCAR:	University Corporation for Atmospheric Research
UCM:	Unresolved Complex Mixture
UCSD:	University of California at San Diego
UHF:	Ultrahigh Frequency
UM:	University of Miami
UNISYS:	United Information Systems
UNOLS:	University-National Oceangraphic Laboratory System
URI:	University of Rhode Island
URSI:	Union Radio Scientifique Internationale
USGS:	United States Geological Survey
UTC:	Coordinated Universal Time
UV:	Ultraviolet
UW:	University of Washington
VAS:	VISSR Atmospheric Sounder
VENTS:	Name of hydrothermal venting research program (not an acronym)
VHF:	Very High Frequency
VICBAR:	Code name for barotropic hurricane track prediction model (not an acronym)
VISSR:	Visible and Infrared Spin-Scan Radiometer
VOC:	Volatile Organic Compound
VOS:	Volunteer Observing Ship
WAM:	Wave Modeling
WATOX:	Western Atlantic Ocean Experiment
WDC:	World Data Center
WEPOCS:	Western Equatorial Pacific Ocean Circulation Study
WHOI:	Woods Hole Oceanographic Institution
WMO:	World Meteorological Organization
WOCE:	World Ocean Circulation Experiment
WOTAN:	Weather Observation Through Ambient Noise
WPL:	Wave Propagation Laboratory (ERL)

WRIPS:	Wave Rider Information Processing System
WSFO:	Weather Service Forecast Office
XBT:	Expendable Bathythermograph

U. S. GOVERNMENT PRINTING OFFICE: 1991--593-7